NMR Studies of Thermo-responsive Poly(asparagine) Derivative

温度応答性ポリアスパラギン誘導体の NMR 研究

Doctor of Engineering

Presented by

Eiji Watanabe

2014

Contents

Chapter 1

General Introduction

Natural polymers such as proteins, polysaccharides, and nucleic acids are found as basic components in living organic systems. Synthetic polymers, which are designed to mimic the biopolymers, have developed into a very active field. These synthetic polymers remain to be the most versatile class of biomaterials owing to the ease in controlling the structures, compositions, and properties. There is a great demand for novel artificial biomaterials with tailored structures and multi-functions.

Historically, natural biopolymer gels have been used as foods and food processing aids as well as in pharmacy. For example, gelatin (a polypeptide obtained from denatured collagen) and agarose (a polysaccharide) showing thermo-reversible gelation have been found. Studies on these gels have been carried out from the viewpoints of structure, gelation processes, and their applications [1−13]. The gelation behavior of natural biopolymers is based on highly cooperative interactions, which can provide driving forces for the responses caused by small environmental changes. For the past several decades, the concept of cooperative interactions between the functional segments of biopolymers has led to the creative idea to invent novel synthetic polymer systems that are environmentally responsive to stimuli [14−17].

Stimuli-responsive polymers are defined as polymers that undergo a

large change in size and physical properties in response to a small external change in the environmental conditions. These polymer systems might recognize a stimulus as a signal, judge the magnitude of this signal, and then change their chain conformation in direct response. These polymers are named ‘smart polymers’ [17]. One approach is to classify the smart polymers according to type of stimuli. The transition behavior of these polymers takes place by changing the thermodynamic or physical field strength. Such changes include temperature, pH, mechanical stress, ionic factor, electric field, magnetic field, and so on (Fig. 1) [14,18−23]. These smart polymers have a wide variety of potentials in bio-related applications.

In a number of smart polymers, thermo-responsive polymers have attracted much attention particularly, because the change of temperature is not only relatively easy to control, but also easily applicable both *in vitro* and *in vivo*. Especially, poly(*N*-isopropylacrylamide) (PNIPAM) is well known that thermo-responsive polymer and have a phase separation temperature (T_{ps}). This PNIPAM aqueous solution has one phase below the T_{ps}, but is phase-separated above the T_{ps}. The reason for this phase separation lies in the balance of hydrophilicity and hydrophobicity in the system. On the basis of the facts that it is important to adjust hydrophilic and hydrophobic balance for developing the transition behavior, various types of thermo-responsive polymers have been designed [21,24−36]. Fig. 2 shows some examples showing a phase transition behavior.

Thermo-responsive hydrogels which are obtained by chemical or physical cross-linking of the thermo-responsive polymers have attracted wide research interest because they exhibit the dramatic change of the dimensions

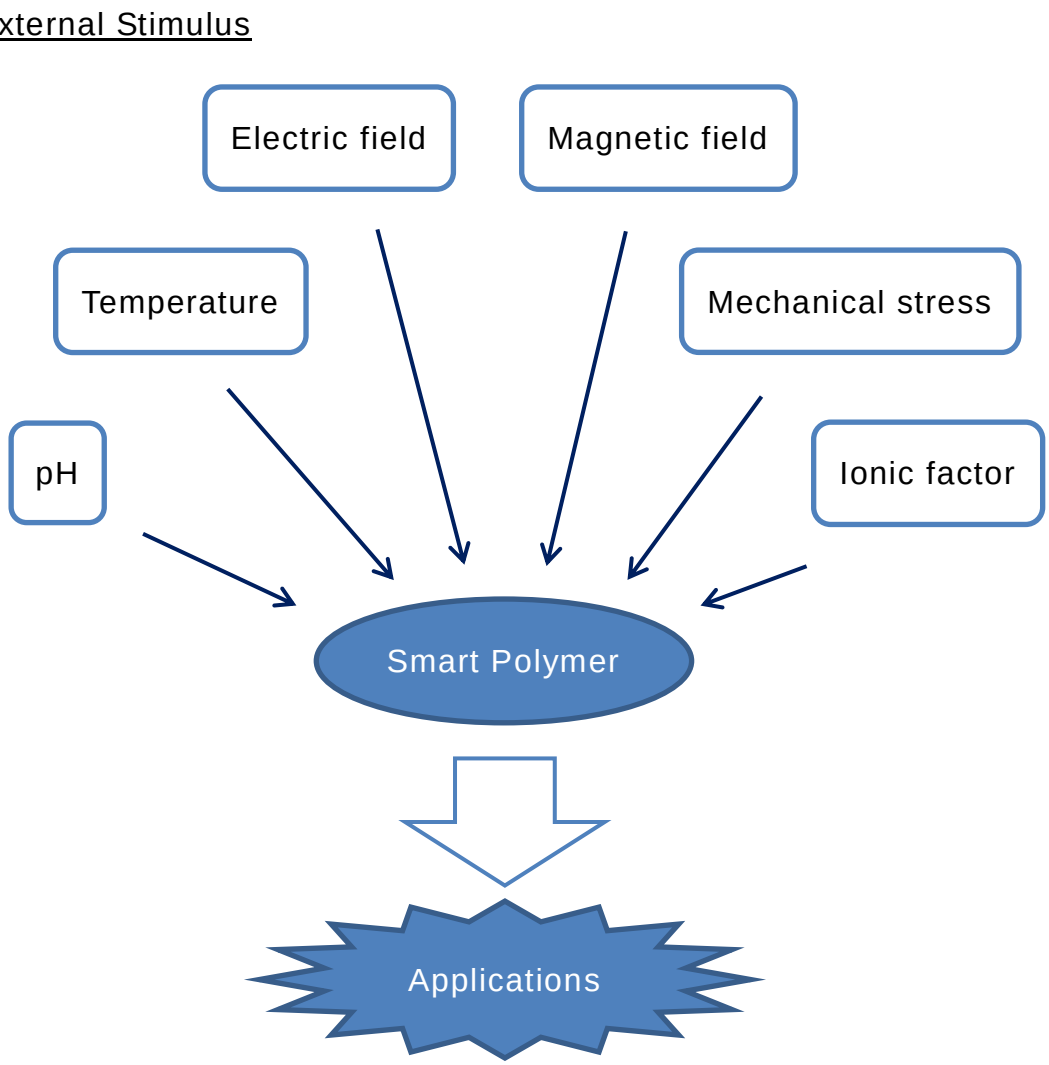

Fig. 1. The schematic image of the stimuli-responsive smart polymer.

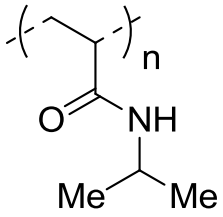

Poly(*N*-isopropylacrylamide)

PNIPAM

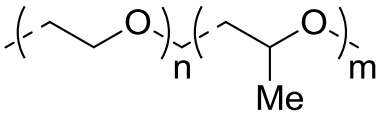

Poly(ethyleneoxide)–*block*–poly(propyleneoxide)

PEO–PPO

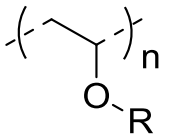

Poly(vinyl ether)s

Fig. 2. The example of well-known thermo-responsive polymers.

of the hydrogels by the temperature change [37−50]. Especially, the structure, physical properties, and the phase transition behaviors of the hydrogels including in a clear lower critical solution temperature (LCST) can be changed by finding out the appropriate balance of hydrophobicity and hydrophilicity and by adjusting the number of electric charges in the chain as well as the degree of cross-linking. Furthermore, hydrogels are polymeric materials that can absorb large amounts of water, while still maintaining a distinct 3-dimensional structure. Hence they can be applied as space filling agents and delivery vehicles for bioactive molecules.

In addition to these thermo-responsive polymers, some of amphiphilic block and graft polymers having thermo-reversible gelation behavior like gelatin have been investigated as novel smart polymers [51−68]. These polymers have a self-assembling property, originated from a hydrophobic effect. They can form polymeric micelles in aqueous solutions. Scheme 1 shows the schematic representation of two different micelle structure transitions following a temperature change at the low and high concentrations of amphiphilic polymers. At the low concentration, polymers in aqueous medium make an isolated micelle structure formation, while, at high concentration, the micelles underwent a network formation, that is, hydrogel. Newly synthesized thermo-reversible gelling polymers have been evaluated according to their characteristics and potential applications.

These smart polymers have important roles as a variety of functional materials, so that many kinds of studies for their synthesis and improvement have been done. This stimuli-responsive system has broadened its usage into different physical forms such as hydrogels, micelles, surfaces, and

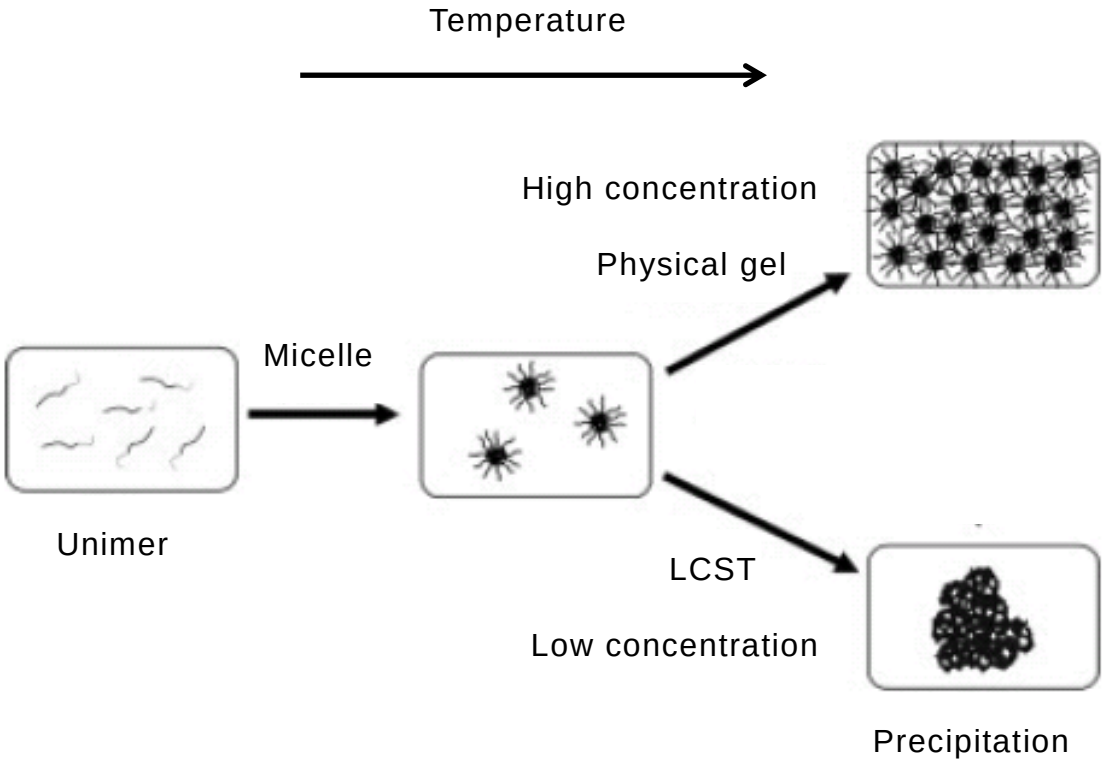

Scheme 1. Schematic diagram of the thermo-responsive polymer in an aqueous solution system.

bioconjugates. Hence, these smart polymers have attracted much attention as versatile bio-related intelligent systems such as gene or drug delivery, chromatography, micro filtration, actuator, sensor, injectable polymeric matrix, and artificial tissue or organs (Fig. 3) [69−80].

As discussed above, the smart polymers are attractive for their potentials of biomaterials. Many researches have been done using the various materials and reactions. However, they have to overcome several barriers: rapid response, mechanical strength, reproductability, biocompatibility, biodegradability, and so on, according to their applications. In particular, biocompatibility and biodegradability should be considered when these polymeric systems are applied into physiological and biological systems.

For device materials in human body, the biocompatibility and complete biodegradability of poly(amino acid)s make them ideal candidates, which are referred to as a small group of polyamides that consist of only one type of amino acid. In addition, amino acids are themselves biologically active, so that it is a great advantage to use amino acids for synthesizing biologically active polymers.

In addition, poly(amino acid)s generate a continuously growing amount of interest and research in medical and pharmaceutical applications because some of these polymers have a potential for chemical modification of existing structures to add desirable segments or functional groups as well as unique properties and functions [81−88]. The ability to selectively place functional groups into the polymer chain permits the control of the custom design of the polymer to tailor its properties for the desired application. Chemical modification of poly(amino acid)s with carboxyl or amino groups

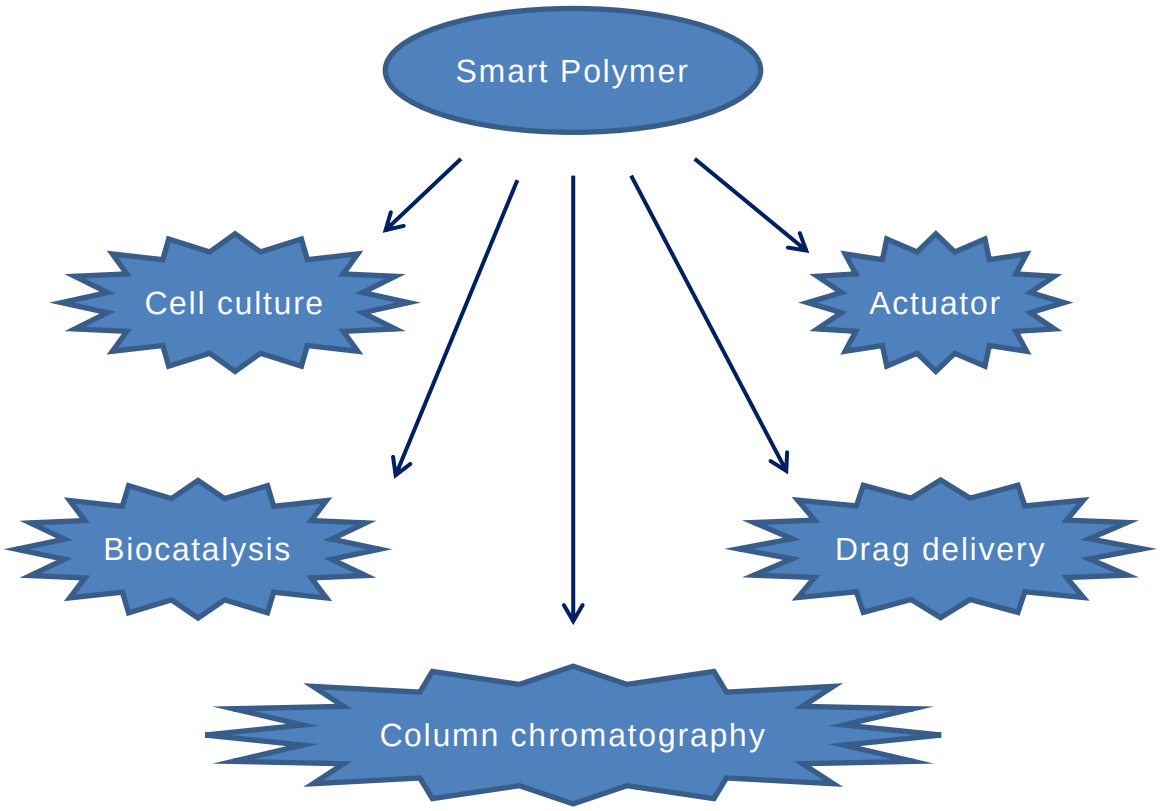

Fig. 3. The schematic image of the use of the stimuli-responsive smart polymer.

seems to be promising as biodegradable polymeric biomaterials because of their own properties. The possibility of applying poly(amino acid)s to biodegradable medical applications such as temporary artificial skin substrates, polymer carriers for protein conjugates and drug delivery systems has been investigated [82,83].

While an increasing number of applications of poly(amino acid)s have been studied, the chemical and bacterial syntheses of poly(amino acid)s were explored as a potential source of new biomaterials. Among them, poly(γ-glutamic acid) (γ-PGA), poly(ε-L-lysine) (ε-PL), and poly(α/β-aspartic acid) (PAA) have become important owing to their unique properties as biopolymers (Fig. 4) [89,90]. These polymers are water-soluble, biodegradable, edible and nontoxic toward humans. Therefore, potential applications of these biopolymer and their derivatives have been of interest in the past few years in a broad range fields such as food, cosmetics, medicine and detergent. In particular, PAA, which can be obtained by mass chemical process such as the alkali hydrolysis of poly(succinimide) (PSI) produced industrially, is expected as applied materials than γ-PGA and ε-PL, which are produced by microbial fermentation [91].

PSI is easy to react with primary amines in mild condition without any condensation agent, thus there were many researches about the poly(aspartic acid) with various side chain groups for biomaterial field [92−107]. Modification of PAA by the copolymerization with other amino acid during polycondensation [108−111] and the polymer grafting [112,113] were also investigated. The gentle biodegradability of thermally synthesized PAA and its derivatives were confirmed by the combination of specific microorganisms,

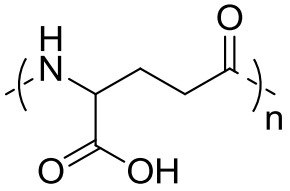

Poly(*γ*-glutamic acid)

γ-PGA

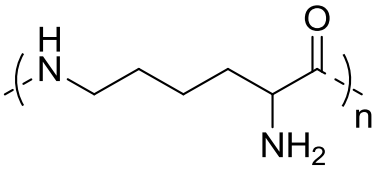

Poly(*ε*-L-lysine)

ε-PL

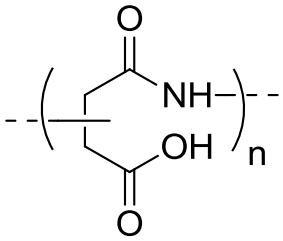

Poly(*α*/*β*-aspartic acid)

PAA

Fig. 4. The some examples of poly(amino acid)s.

such as *Pedobacter* sp. KP-2 and *Sphingomonas* sp. KT-l [114−118]. Furthermore, PAA is expected as a good candidate for the replacement of nonbiodegradable poly(acrylic acid)s in many fields of applications, such as builder and dispersant in detergent, chelating agents in wastewater treatment, paper additive, and superabsorbent polymer.

Along with an increasing number of applications, a growing demand for polymeric materials possessing multiple functions will most probably expand more rapidly for the next decades. Concerning the use of these polymers in human body, biocompatibility and biodegradability of the main chain are an important factor. Novel functional materials of unique properties having stimuli-responsive behavior would be designed and evaluated by the chemical modification of poly(amino acid)s.

With the background described above, the present thesis consists of three chapters including the following topics on the development of novel thermo-responsive polymers based on PAA derivatives for construction of biodegradable smart materials.

In Chapter 2, the preparation of thermo-responsive biodegradable polymers from PSI is described. Reaction of PSI with hydrophilic and hydrophobic amines produced new biodegradable polymers, poly(*N*-substituted *α*/*β*-asparagine) derivatives (PADs), showing the LCST and the sol−gel−sol phase transition behavior in water (Scheme 2). The effect of the composition ratio of the side chain on the LCST and the gelation temperature was investigated by dynamic viscoelastic measurement. Furthermore, the sol−gel−sol phase transition mechanism in these polymer systems was revealed by measurements of the particle size at each temperature

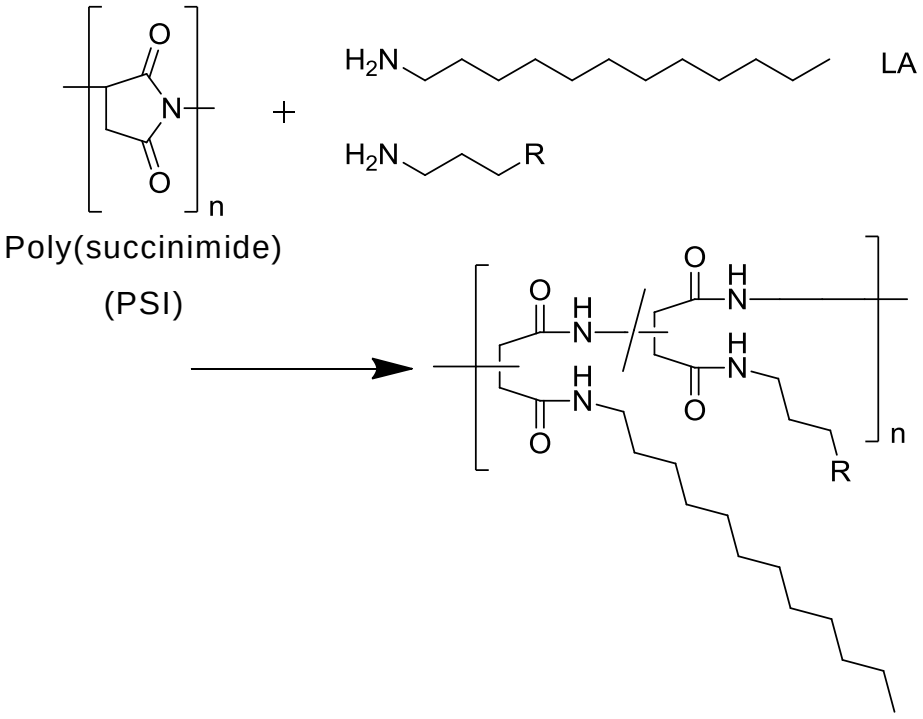

Scheme 2. The thermo-responsive poly(*N*-substituted *α*/*β*-asparagine) derivatives (PADs); R = $-N(CH_3)_2$ or –OH.

and transmission electron microscope photos of each phase.

In Chapter 3, the detailed structural characterization of this thermo-responsive and biodegradable PAD with the hydroxyl group in the terminal moieties of the hydrophilic side chains in water was investigated using ^{1}H and ^{13}C solution NMR spectroscopy.

In Chapter 4, the complex aggregation and dissociation process resulting in the sol to gel transition of thermo-responsive PAD aqueous solution was studied by using several NMR methods (Fig. 5). Both ^{13}C solution and solid state cross polarization / magic angle spinning NMR approaches were used to study the structure and dynamics of PAD molecules. In addition, deuterium two-dimensional (2D) T_1-T_2 and T_2-T_2 relaxation spectroscopies, based on an inverse Laplace transform (ILT), were used to monitor the distribution, dynamics, and exchange of water in the PAD−water mixture during the phase transition. Molecular motion in this system, during thermo-responsive behavior occurs, is elucidated. The application of these 2D ILT maps of T_1 and T_2 relaxation times to thermo-responsive polymer aqueous solution is relatively new experimental technique.

These investigations provide the synthesis of novel functional polymers based on poly(amino acid)s. Various applications of these polymers can be expected in the biomedical field and so on. The experimental results are described in the following chapters.

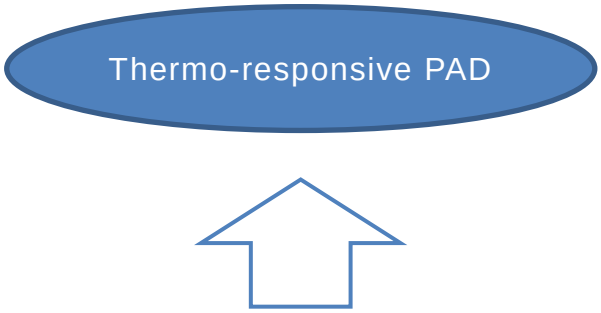

1. Primary Structure of PAD in water
   → ^{13}C solution NMR

2. Structural feature of PAD in water with heating
   → ^{13}C solution NMR and ^{13}C CP/MAS NMR

3. Structural feature of water molecules with heating
   → ^{2}H 2D T_1–T_2 and T_2–T_2 relaxation spectroscopy

Fig. 5. Analysis strategy of thermo-responsive mechanism of PADs in an aqueous solution.

References

[1] S.-H. Hsu, A. M. Jamieson, *Polymer*, 34 (1993) 2602.

[2] L. Picullel, B. Lindman, *Adv. Colloid Interface Sci.*, 41 (1992) 149.

[3] W. F. Harrington, N. V. Rao, *Biochemistry*, 9 (1970) 3714.

[4] M. Djabourov, J. Leblond, P. Papon, *J. Phys. (Paris)*, 49 (1988) 333.

[5] K. Nijenhuis, *Colloid Polym. Sci.*, 259 (1981) 522.

[6] G. Cuvelier, B. Launay, *Macromol. Chem. Macromol. Symp.*, 40 (1990) 23.

[7] E. J. Amis, D. F. Hodgson, Q. Yu, *Polym. Prepr.*, 32 (1991) 447.

[8] H. Huang, C. M. Sorensen, *Phys. Rev. E*, 53 (1996) 5075.

[9] J. Peyrelasse, M. Lamarque, J. P. Habas, H. Boedtkaer, N. E. Bounia, *Phys. Rev. E*, 53 (1996) 6126.

[10] C. Michon, G. Cuvelier, B. Launay, *Rheol. Acta*, 32 (1993) 94.

[11] M. Okamoto, T. Norisuye, M. Shibayama, *Macromolecules*, 34 (2001) 8496.

[12] V. Crescenzi, A. Francescangeli, A. Taglienti, *Biomacromolecules*, 3 (2002) 1384.

[13] T. Silva, A. Kirkpatrick, B. Brodsky, J. A. M. Ramshaw, *J. Agric. Food Chem.*, 53 (2005) 7802.

[14] P. Gupta, K. Vermani, S. Garg, *Drug. Discov. Today*, 7 (2002) 569.

[15] B. Jeong, A. Gutowska, *Trends. Biotechnol.*, 20 (2002) 305.

[16] E. S. Gil, S. M. Hudson, *Prog. Polym. Sci.*, 29 (2004) 1173.

[17] A. S. Hoffman, P. S. Stayton, V. Bulmus, G. Chen, J. Chen, C. Cheung, A. Chilkoti, Z. Ding, L. Dong, R. Fong, C. A. Lackey, C. J. Long, M.

Miura, J. E. Morris, N. Murthy, Y. Nabeshima, T. G. Park, O. W. Press, T. Shimoboji, S. Shoemaker, H. J. Yang, N. Monji, R. C. Nowinski, C. A. Cole, J. H. Priest, J. M. Harris, K. Nakamae, T. Nishino, T. Miyata, *J. Biomed. Mater. Res.*, 52 (2000) 577.

[18] J. G. Noh, Y. J. Sung, K. E. Geckeler, S. E. Kudaibergenov, *Polymer*, 46 (2005) 2183.

[19] Z. Megeed, J. Cappello, H. Ghandehari, *Adv. Drug Deliv. Rev.*, 54 (2002) 1075.

[20] O. Braun, J. Selb, F. Candau, *Polymer*, 42 (2001) 8499.

[21] F. Bignotti, M. Penco, L. Sartore, I. Peroni, R. Mendichi, M. Casolaro, A. D'Amore, *Polymer*, 41 (2000) 8247.

[22] A. Izumi, R. Nomura, T. Masuda, *Macromolecules*, 34 (2001) 4342.

[23] A. M. Granville,S. G. Boyes, B. Akgun, M. D. Foster, W. J. Brittain, *Macromolecules*, 37 (2004) 2790.

[24] L. D. Taylor, L. D. Cerankowski, *J. Polym. Sci.*, 13 (1975) 2551.

[25] X. Li, W. Liu, G. Ye, B. Zhang, D. Zhu, K. Yao, Z. Liu, X. Sheng, *Biomaterials*, 26 (2005) 7002.

[26] M. Yoshida, M. Asano, S. Safranj, H. Omichi, R. Spohr, J. Vetter, R. Katakai, *Macromolecules*, 29 (1996) 8987.

[27] H. Katono, A. Maruyama, N. Ogata, K. Sanui, T. Okano, Y. Sakurai, *J. Control. Release*, 16 (1991) 215.

[28] T. Okano, Y. H. Bae, S. W. Kim, *J. Control. Release*, 11 (1990) 255.

[29] N. Monji, A. S. Hoffman, *Appl. Biochem. Biotechnol.*, 14 (1987) 107.

[30] T. G. Park, A. S. Hoffman, *Appl. Biochem. Biotechnol.*, 19 (1988) 1.

[31] M. Okubo, H. Ahmad, T. Suzuki, *Colloid. Polym. Sci.*, 276 (1998)

470.

[32] K. Suwa, K. Yamamoto, M. Akashi, K. Takano, N. Tanaka, S. Kunugi, *Colloid. Polym. Sci.*, 276 (1998) 529.

[33] Y. Maeda, *Langmuir*, 17 (2001) 1737.

[34] S. Hasegawa, H. Ohashi, Y. Maekawa, R. Katakai, M. Yoshida, *Radi. Phys. and Chem.*, 72 (2005) 595.

[35] J. Reguera, M. Alonso, A. M. Testera, I. M. López, S. Martín, J. C. Rodríguez-Cabello, *Carbo. Polym.*, 57 (2004) 293.

[36] D. Christova, R. Velichkova, W. Loos, E. J. Goethals, F. D. Prez, *Polymer*, 44 (2003) 2255.

[37] M. Higa, T. Yamakawa, *J. Phys. Chem. B.*, 108 (2004) 16703.

[38] K. Suzuki, T. Yumura, Y. Tanaka, M. Akashi, *J. Control. Release*, 75 (2001) 183.

[39] Q. Sun, Y. Deng, *Langmuir*, 21 (2005) 5812.

[40] K. Durme, B. Mele, W. Loos, F. E. Prez, *Polymer*, 46 (2005) 9851.

[41] M. Panayiotou, R. Freitag, *Polymer*, 46 (2005) 6777.

[42] A. Matsumoto, T. Kurata, D. Shiino, K. Kataoka, *Macromolecules*, 37 (2004) 1502.

[43] M. Annaka, T. Matsuura, M. Kasai, T. Nakahira, Y. Hara, T. Okano, *Biomacromolecules*, 4 (2003) 395.

[44] X. Zhang, D. Wu, C. C. Chu, *Biomaterials*, 25 (2004) 4719.

[45] A. N. Nedelcheva, C. P. Novakov, S. M. Miloshev, I. V. Berlinova, *Polymer*, 46 (2005) 2059.

[46] S. I. Kang, Y. H. Bae, *Macromolecules*, 34 (2001) 8173.

[47] K. Trabbic-Carlson, L. A. Setton, A. Chilkoti, *Biomacromolecules*, 4

(2003) 572.

[48] M. Higa, T. Yamakawa, *J. Phys. Chem. B.*, 109 (2005) 11373.

[49] V. Grabstain, H. Bianco-Peled, *Biotechnol. Prog.*, 19 (2003) 1728.

[50] J. D. Debord, L. A. Lyon, *Langmuir*, 19 (2003) 7662.

[51] D. Schmaljohann, J. Oswald, B. Jorgensen, M. Nitschke, D. Beyerlein, C. Werner, *Biomacromolecules*, 4 (2003) 1733.

[52] M. D. C. Topp, P. J. Dijkstra, H. Talsma, J. Feijen, *Macromolecules*, 30 (1997) 8518.

[53] J. Virtanen, S. Holappa, H. Lemmetyinen, H. Tenhu, *Macromolecules*, 35 (2002) 4763.

[54] J. E. Chung, M. Yokoyama, T. Okano, *J. Control. Release*, 65 (2000) 93.

[55] F. Kohori, K. Sakai, T. Aoyagi, M. Yokoyama, Y. Sakurai, T. Okano, *J. Control. Release*, 55 (1998) 87.

[56] H. Miyazaki, K. Kataoka, *Polymer*, 37 (1996) 681.

[57] D. Neradovic, C. F. Nostrum, W. E. Hennink, *Macromolecules*, 34 (2001) 7589.

[58] D. Duracher, S. A. Ela, F. Mallet, C. A. Pichot, *Langmuir*, 16 (2000) 9002.

[59] J. E. Chung, M. Yokoyama, T. Aoyagi, Y. Sakurai, T. Okano, *J. Control. Release*, 53 (1998) 119.

[60] P. M. Pakhomov, S. Khizhnyak, E. Ruhl, V. Egorov, A. Tshmel, *Eur. Polym. J.*, 39 (2003) 1019.

[61] Z. Ding, G. Chen, A. S. Hoffman, *J. Biomed. Mater. Res.*, 39 (1998) 498.

[62] A. Au, J. Ha, A. Polotsky, K. Krzyminski, A. Gutowska, D. S. Hungerford, C. G. Frondoza, *J. Biomed. Mater. Res. A*, 67 (2003) 1310.

[63] P. Pakhomov, S. Khizhnyak, K. Kober, A. Tshmel, *Eur. Polym. J.*, 37 (2001) 623.

[64] K. Park, K. Na, S. Y. Jung, S. W. Kim, K. H. Park, K. Y. Cha, H. M. Chung, *J. Biosci. Bioengi.*, 99 (2005) 598.

[65] A. Safrany, *Radi. Phys. and Chem.*, 55 (1999) 121.

[66] F. Kohori, M. Yokoyama, K. Sakai, T. Okano, *J. Control. Release*, 78 (2002) 155.

[67] D. E. Meyer, B. C. Shin, G. A. Kong, M. W. Dewhirst, A. I. Chilkoti, *J. Control. Release*, 74 (2001) 213.

[68] T. Takezawa, Y. Mori, K. Yoshizato, *Biotechnology*, 8 (1990) 854.

[69] X. S. Wu, A. S. Hoffman, P. Yager, *J. Polym. Sci. Part A: Polym. Chem.*, 30 (1992) 2121.

[70] Y. H. Lim, D. Kim, D. S. Lee, *J. Appl. Polym. Sci.*, 64 (1997) 2647.

[71] Y. Qiu, K. Park, *Adv. Drug Deliv. Rev.*, 53 (2001) 321.

[72] S. Sharma, P. Kaur, A. Jain, M. R. Rajeswari, M. N. Gupta, *Biomacromolecules*, 4 (2003) 330.

[73] A. Chilkoti, M. R. Dreher, D. E. Meyer, D. Raucher, *Adv. Drug Deliv. Rev.*, 54 (2002) 613.

[74] J. Kobayashi, A. Kikuchi, K. Sakai, T. Okano, *J. Chromatogr. A*, 958 (2002) 109.

[75] I. Y. Galaev, B. Mattiasson, *Enzyme. Microb. Technol.*, 15 (1993) 354.

[76] S. Sershen, J. West, *Adv. Drug Deliv. Rev.*, 54 (2002) 1225.

[77] J. Z. Wu, A. P. Sassi, H. W. Blanch, J. M. Prausnitz, *Polymer*, 37 (1996) 4803.

[78] M. Yokoyama, *Drug. Discov. Today*, 2002, 7, 426.

[79] L. E. Bromberg, E. S. Ron, *Adv. Drug Deliv. Rev.*, 31 (1998) 197.

[80] J. Weidner, *Drug. Discov. Today*, 6 (2001) 1239.

[81] D. Jermakowicz-Bartkowiak, B. N. Kolarz, A. Serwin, *Reac. Functi. Polym.*, 65 (2005) 135.

[82] A. Lavasanifar, J. Samuel, G. S. Kwon, *Adv. Drug Deliv. Rev.*, 54 (2002) 169.

[83] R. Fernández-Lafuente, V. Rodríguez, C. Mateo, G. Fernández-Lorente, P. Arminsen, P. Sabuquillo, J. M. Guisán, *J. Mol. Cat. B: Enzym.*, 7 (1999) 173.

[84] R. Bahulekar, N. Tamura, S. Ito, M. Kodama, *Biomaterials*, 20 (1999) 357.

[85] F. Rypačk, *Polym. Degrad. Stab.*, 59 (1998) 345.

[86] A. Gupta, P. Tandon, V. Dayal, S. Rastogi, *Polymer*, 38 (1997) 2389.

[87] L. C. Petersen, E. Suenson, *Biochim. Biophys. Acta*, 883 (1986) 313.

[88] B. Romberg, J. M. Metselaar, T. de Vringer, K. Motonaga, J. J. Kettenes-van den Bosch, C. Oussoren, G. Storm, W. E. Hennink, *Bioconjugate Chem.*, 16 (2005) 767.

[89] M. Obst, A. Steinbüchel, *Biomacromolecules*, 5 (2004) 1166.

[90] F. B. Oppermann-Sanio, A. Steinbüchel, *Naturwissenschaften*, 89 (2002) 11.

[91] S. Roweton, S. J. Huang, G. Swift, *J. Environ. Polym. Degrad.*, 5 (1997) 175.

[92] J. Filipović-Grčić, D. Maysinger, B. Zorc, I. Jašenjak, *Int. J. Pharm.*, 116 (1995) 39.

[93] G. Spadaro, C. Dispenza, G. Giammona, G. Pitarresi, G. Cavallaro, *Biomoterials*, 17 (1996) 953.

[94] G. Giammona, G. Pitarresi, G. Cavallaro, S. Buscemi, F. Saiano, *Biochim. Biophys. Acta*, 1428 (1999) 29.

[95] G. Giammona, G. Cavallaro, G. Pitarresi, *Adv. Drug Deliv. Rev.*, 39 (1999) 153.

[96] G. Pitarresi, G. Cavallaro, B. Carlisi, G. Giammona, D. Bulone, P. L. S. Biagio, *Macromol. Chem. Phys.*, 201 (2000) 2542.

[97] H. S. Kang, M.-S. Shin, J.-D. Kim, J.-W. Yang, *Polym. Bull.*, 45 (2000) 39.

[98] P. Caliceti, S. M. Quarta, F. M. Veronese, G. Cavallaro, E. Pedone, G. Giammona, *Biochim. Biophys. Acta*, 1528 (2001) 177.

[99] H. S. Kang, S. R. Yang, J.-D. Kim, S.-H. Han, I.-S. Chang, *Langmuir*, 17 (2001) 7501.

[100] M. G. Meirim, E. W. Neuse, D. D. N'da, *J. Appl. Polym. Sci.*, 82 (2001) 1844.

[101] G. Pitarresi, P. Pierro, G. Giammona, F. Iemma, R. Muzzalupo, N. Picci, *Biomaterials*, 25 (2004) 4333.

[102] H. Chen, W. Xu, T. Chen, W. Yang, J. Hu, C. Wang, *Polymer*, 46 (2005) 1821.

[103] G.-P. Yan, M.-L. Liu, L.-Y. Li, *Bioconjugate Chem.*, 16 (2005) 967.

[104] M. B. Biličić, J. Filipović-Grčić, A. Martinac, M. Barbarić, B. Zorc, B. Cetina-Čižmek, P. Tudja, *Int. J. Pharm.*, 291 (2005) 211.

[105] M. Licciardi, M. Campisi, G. Cavallaro, M. Cervello, A. Azzolina, G. Giammona, *Biomaterials*, 27 (2006) 2066.

[106] G. Pitarresi, F. S. Palumbo, A. Albanese, M. Licciardi, F. Calascibetta, G. Giammona, *Eur. Polym. J.*, 44 (2008) 3764.

[107] E. F. Craparo, G. Pitarresi, M. L. Bondí, M. P. Casaletto, M. Licciardi, G. Giammona, *Macromol. Biosci.*, 8 (2008) 247.

[108] M. Tomida, T. Nakato, M. Kuramochi, M. Shibata, S. Matsunami, T. Kakuchi, *Polymer*, 37 (1996) 4435.

[109] T. Kakuchi, M. Shibata, S. Matsunami, T. Nakato, M. Tomida, *J. Polym. Sci. Part A: Polym. Chem.*, 35 (1997) 285.

[110] G. Tang, B. He, *J. Appl. Polym. Sci.*, 102 (2006) 46.

[111] H. Shinoda, Y. Asou, A. Suetsugu, K. Tanaka, *Macromol. Biosci.*, 3 (2003) 34.

[112] J. H. Jeong, H. S. Kang, S. R. Yang, J.-D. Kim, *Polymer*, 44 (2003) 583.

[113] H. J. Lee, S. R. Yang, E. J. An, J.-D. Kim, *Macromolecules*, 39 (2006) 4938.

[114] D. D. Alford, A. P. Wheeler, C. A. Pettigrew, *J. Environ. Polym. Degrad.*, 2 (1994) 225.

[115] K. Tabata, H. Abe, Y. Doi, *Biomacromolecules*, 1 (2000) 157.

[116] K. Tabata, M. Kajiyama, T. Hiraishi, H. Abe, I. Yamato, Y. Doi *Biomacromolecules*, 2 (2001) 1155.

[117] T. Hiraishi, M. Kajiyama, K. Tabata, I. Yamato, Y. Doi, *Biomacromolecules*, 4 (2003) 80.

[118] T. Hiraishi, M. Kajiyama, K. Tabata, H. Abe, I. Yamato, Y. Doi,

Biomacromolecules, 4 (2003) 1285.

Chapter 2

Preparation and Physical Properties of Thermo-responsive Poly(asparagine) Derivatives

1. Introduction

Recently, there has been great interest in polymers exhibiting the phase transition that is readily reversible with thermal stimulus. Among them, poly(*N*-isopropylacrylamide) (PNIPAM) is currently the most extensively studied thermo-responsive polymer [1−3]. PNIPAM, NIPAM-containing copolymers, and PNIPAM-based cross-linked hydrogels have been widely applied to controlled drug delivery, biomedical materials, fillers of column chromatography, gene-transfection agents, immobilized biocatalysts, and others [4−10]. However, non-biodegradability of PNIPAM may restrict its applications in the biomedical field. It was reported that aqueous solutions of block copolymers of biodegradable poly(lactic acid)−poly(ethylene glycol)showed the sol−gel transition [11]. Amphiphilic block copolymers showing thermo-gelation upon heating were reported. Typical examples are poly(ethylene glycol)−*block*−poly(propylene glycol) and poly(2-(2-ethoxy)ethoxyethyl vinyl ether)−*block*−poly(2-methoxyethyl vinyl ether) [12,13].

Poly(amino acid)s are biodegradable and biocompatible materials,

useful for various bio-related industries [14]. Poly(*α*/*β*-aspartic acid), which is synthesized by thermal polymerization of aspartic acid, followed by alkaline hydrolysis, is expected to be an alternative to non-biodegradable poly(acrylic acid) widely used in various industrial fields. Recently, it was reported that the poly(aspartic acid) derivatives formed the micelle in the aqueous solution, and new thermo-responsive polymers based on biodegradable poly(amino acid)s, poly(*N*-substituted *α*/*β*-asparagine)s, which showed a clear lower critical solution temperature (LCST) in water, have been developed [15−18]. However, these thermo-responsive poly(asparagine)s did not show a sol−gel−sol phase transition in water.

This chapter deals with new amphiphilic poly(*N*-substituted *α*/*β*-asparagine) derivatives (PADs) showing sharp thermo-responsive properties. By precise control of the introduction of the hydrophilic and the hydrophobic group into the side chain of poly(*α*/*β*-asparagine)s [19,20], not only demonstrated a phase separation in a dilute aqueous solution but also a physical gelation in a concentrated aqueous solution.

2. Experimental section

2.1. General procedure of preparation of thermo-responsive PADs

A typical preparation of thermo-responsive PAD was as follows (Fig. 1). Poly(succinimide) (PSI) (**1**) with M_w and $M_w = M_n$ of 9.8×10^4 and 1.45, respectively, was used as a precursor. Poly(succinimide) (PSI) (**1**) (9.7 g, 0.1 mol) was dissolved in *N*,*N*-dimethylformamide (DMF) (34 g) in a separable flask equipped with a mechanical stirrer and a thermometer. A mixture of dodecylamine (LA) (6.5 g, 0.035 mol) and *N*,*N*-dimethyl-1,3-propanediamine (DMPDA) (6.6 g, 0.065 mol) was added. The reaction mixture was kept at 70 ˚C for 6 hours, in which the succinimide group of **1** was quantitatively reacted to form a *N*-substituted asparagine unit. The resulting solution was poured into a large amount of acetone. The formed precipitates were collected by filtration and dried at 60 ˚C for 24 hours (20.9 g, 92 % yield). The content of LA and DMPDA in the polymer was determined by ^{1}H NMR spectroscopy. The composition of the side chain in PAD was determined by the integrated ratio of peaks of methyl protons of the dodecyl group (3H, t, 0.89 ppm) and central methylene protons derived from DMPDA (2H, b, 1.71 ppm) in the ^{1}H NMR spectrum of **2a−e**. In the case of using 3-amino-1-propanol (AP) as hydrophilic amine, the composition of the side chain in PAD was determined by the integrated ratio of peak of central methylene protons derived from AP (2H, b, 1.55 ppm) in the ^{1}H NMR spectrum of **3a−d**. All other polymers were obtained in the same manner.

In this chapter, nine polymer samples with different hydrophilic

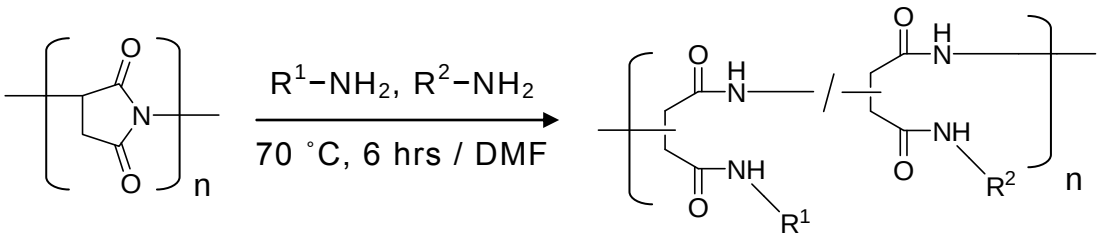

Poly(succinimide)

(PSI: **1**)

Poly(*N*-substituted *α*/*β*-asparagine) derivative

(PAD: **2a**−**e**, **3a**−**d**)

R^1: $-(CH_2)_{11}CH_3$

R^2: $-(CH_2)_3N(CH_3)_2$, $-(CH_2)_3OH$

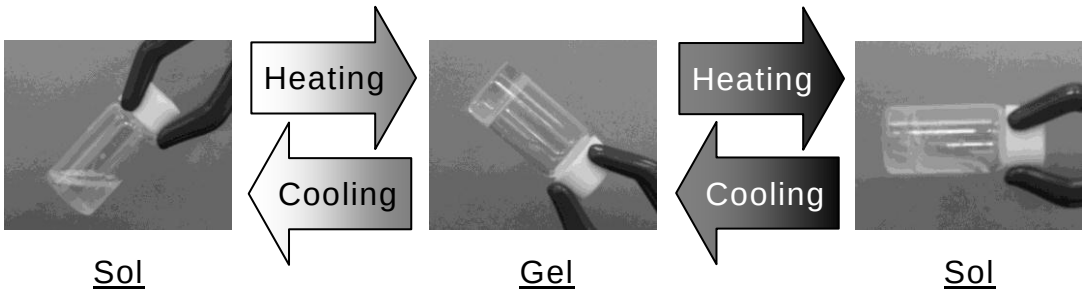

Fig. 1. Preparation and a sol−gel−sol phase transition of thermo-responsive poly(*N*-substituted *α*/*β*-asparagine) derivatives (PADs).

amines and/or different LA content were synthesized. Table 1 summarizes their composition ratio and physical properties. All of these polymers were soluble in water at low temperature. On the other hand, the PAD with the LA content higher than 58 % was not soluble in water, even at 5 ˚C.

2.2. Physical properties

The dynamic viscosity of the PAD aqueous solutions was measured using a stress-control rheometer (Viscoanalyzer Var-50/100, Reologica Instrument, AB) equipped with a parallel plate geometry (40 mm diameter) at a heating ratio of 1.0 ˚C/min at a constant frequency (1.0 Hz). The temperature in all viscosity measurements was controlled to within 0.1 ˚C by a Peltier element.

2.3. Lower critical solution temperature (LCST) determination

To determine a LCST, aqueous solutions of 1.0 wt% thermo-responsive PADs were prepared in distilled water. LCST was measured by UV-vis spectroscopy (UV-2500PC equipped with a Peltier-type thermo-static cell holder PC-TEC controller, Shimadzu) to determine the turbidity of the solutions at 500 nm. The heating rate of the cell was adjusted at 1.0 ˚C/min. The LCST was defined as 50 % transmittance of polymer solution during the heating process.

Table 1. Composition ratio and physical properties of synthesized PADs.

Sample	R^1	R^2	R^1/R^2 [a]	Gelation [b]		LCST [c]
				T_{sg} / °C [d]	T_{gs} / °C [e]	T_{ps} / °C [f]
2a	$-(CH_2)_{11}CH_3$	$-(CH_2)_3N(CH_3)_2$	27/73	−	−	78
2b	↑	↑	37/63	−	−	56
2c	↑	↑	42/58	−	−	44
2d	↑	↑	48/52	18	39	28
2e	↑	↑	52/48	10	35	−
3a	↑	$-(CH_2)_3OH$	50/50	18	52	−
3b	↑	↑	45/55	29	61	−
3c	↑	↑	40/60	44	54	−
3d	↑	↑	35/65	−	−	−

a) Determined by ^{1}H NMR;

b) Measured with the 10 wt% polymer aqueous solutions;

c) Measured with the 1.0 wt% polymer aqueous solutions;

d) Transition temperature from sol to gel phase;

e) Transition temperature from gel to sol phase.

f) Phase separation temperature defined as 50 % transmittance of polymer solution during the heating process.

2.4. Dynamic light scattering (DLS) measurements

The DLS (Zetasizer Nano ZS, Malvern) measurements were carried out with 1.0 wt% PAD aqueous solution as a function temperature in a range of 10−75 ˚C with an increment 5 ˚C each step. All solutions were equilibrated for 7 min at each measured temperature before the measurement. Measurements of scattered light were made at an angle 90 ˚ to the incident beam. The results of DLS were analyzed by the regularized CONTIN method. The decay rate distributions were transformed to an apparent diffusion coefficient. From the diffusion coefficient, the apparent hydrodynamic size of a polymer aggregate can be obtained by the Stokes−Einstein equation.

2.5. Transmission electron microscopy (TEM)

The microscopic image was obtained by negative staining using uranyl acetate with an accelerating voltage of 100 kV (JEM-1011, JEOL). A typical TEM grid preparation was as follows: the PAD aqueous solutions were diluted with Milli-Q water to approximately 0.01 wt%, and kept for 30 min at measured temperature.

3. Results and discussion

3.1. Thermo-responsive PAD using DMPDA as hydrophilic group

3.1.1. Physical properties

Fig. 2 shows the temperature dependence of the viscosity of 10 wt% aqueous solutions of polymers **2c**, **2d**, and **2e** on the heating process in the temperature range from 5 ˚C to 80 ˚C. Polymer **2e** showed a significant increase in viscosity, and the maximum viscosity of polymer **2e** was observed at 24 ˚C. Around this temperature, the solution apparently turned into a gel due to the very high viscosity. Above this temperature, the viscosity rapidly decreased. Similar behavior was observed in polymers **2c** and **2d**. As the LA content in polymers **2c**, **2d**, and **2e** increased, the temperature of the maximum viscosity decreased and the maximum viscosity increased. On the other hand, only a very small change in the viscosity was seen in polymer **2b**, and the viscosity of polymer **2a** scarcely changed in the temperatures measured.

In order to elucidate the present thermo-gelation behavior, the dynamic viscoelasticity of the polymer solution was measured. Fig. 3 depicted traces of storage modulus (G’), loss modulus (G’’), and tan δ of 10 wt% solution of polymer **2d**. Below 18 ˚C, G’’ was larger than G’ (G’’ > G’). This confirmed that the polymer solution behaves like sol below this temperature. At 18 ˚C, the G’ value suddenly increased to the same as G’’ (G’’ = G’, tan δ = 1), indicating that the phase transition from sol-like elasticity-state to gel-like viscosity-state (sol−gel phase transition) took place. In the range from 18 ˚C

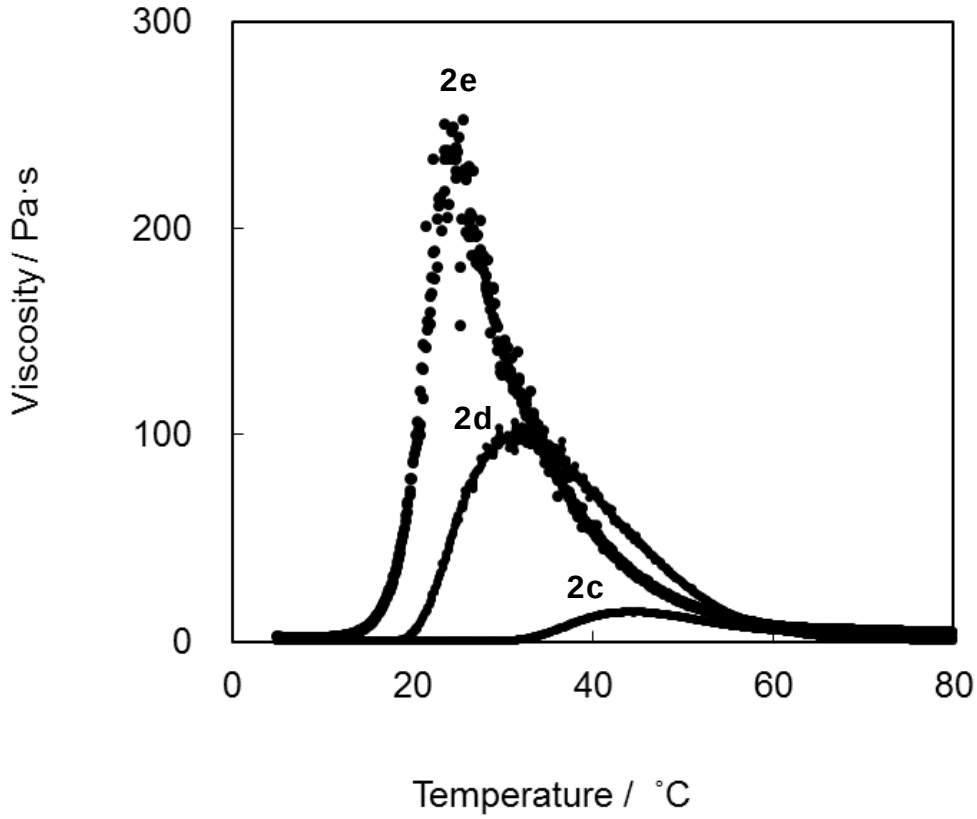

Fig. 2. Temperature dependence of apparent viscosity for 10 wt% PAD aqueous solutions (polymers **2c**–**e**).

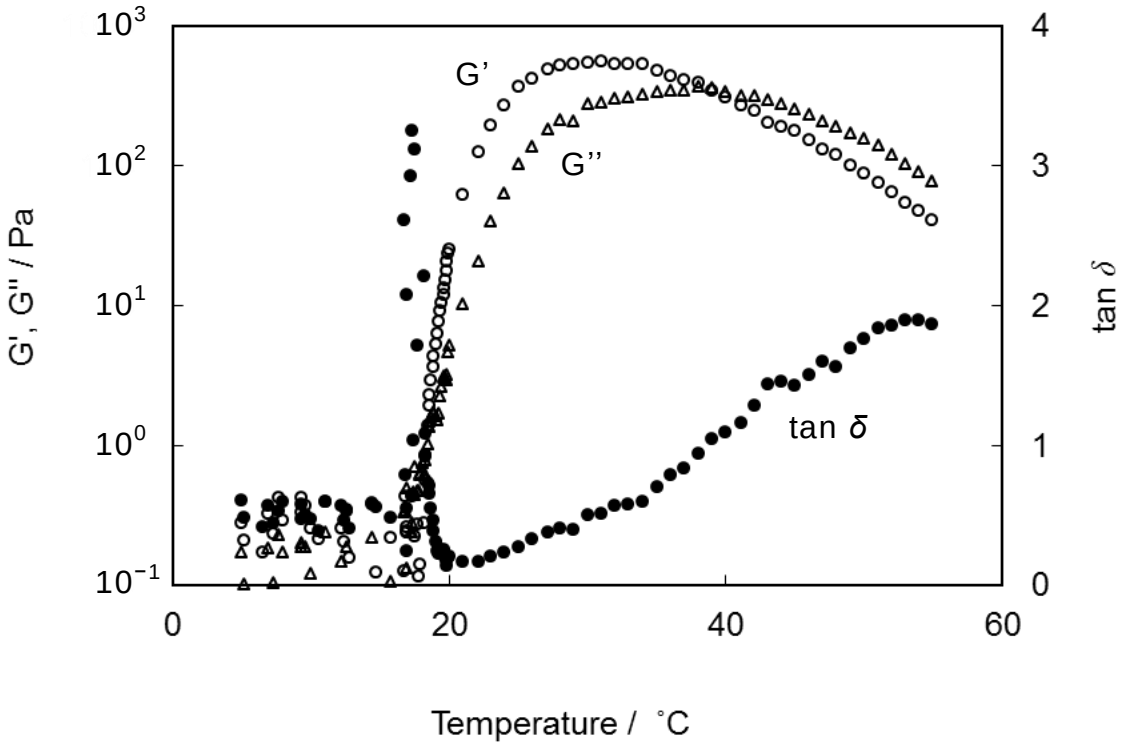

Fig. 3. Temperature dependence of storage modulus (G’), loss modulus (G’’) and tan δ for 10 wt% polymer **2d** aqueous solution.

to 39 ˚C, the gel phase (G'' < G') was observed. Above 39 ˚C, the order was reversed again (G'' > G'), at which the gel phase returned to the sol phase (gel−sol phase transition). These phenomena clearly showed a sol−gel−sol phase transition of polymer **2d** with thermal stimulus. In the case of polymer **2e**, the sol−gel phase transition occurred at 10 ˚C and the gel−sol phase transition occurred at 35 ˚C. For polymer **2c**, G' was smaller than G'' (G'' > G') in the region of all the temperatures examined, although a viscosity increase was observed. The same relation between G' and G'' was also seen in polymers **2a** and **2b**. These data suggested that the gel phase was not observed in polymer **2a**, **2b**, and **2c**.

3.1.2. Phase separation behavior

Moreover, these polymer solutions of the dilute concentration exhibited not only a sol−gel−sol phase transition but also the thermally responsive phase separation. Fig. 4 shows the temperature dependence of a light beam transmittance of 1.0 wt% aqueous solutions of polymers **2a–d** at 500 nm on the heating process. For all the samples, the turbidity change took place sharply. In the cooling process, similar behavior was observed. Temperature at 50 % of transmittance on the heating process is defined as the LCST (T_{ps}). As the content of the hydrophobic substituent (LA) increased, the T_{ps} decreased. By changing the composition ratio of LA and DMPDA in PAD, T_{ps} could be accurately controlled over a wide range from room temperature to around 80 ˚C. The LCST was in the wide range from room temperature to the approximate boiling point of water and linearly increased as a function of

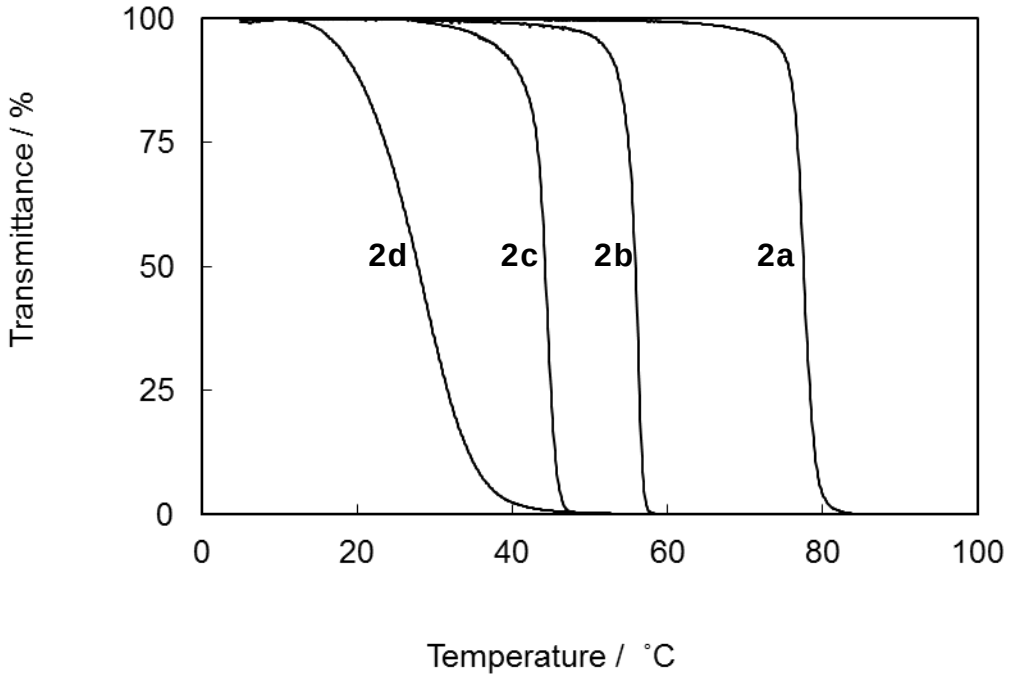

Fig. 4. Temperature dependence of light beam transmittance on heating process; 1.0 wt% aqueous solution, wavelength = 500 nm, heating rate = 1.0 ˚C/min.

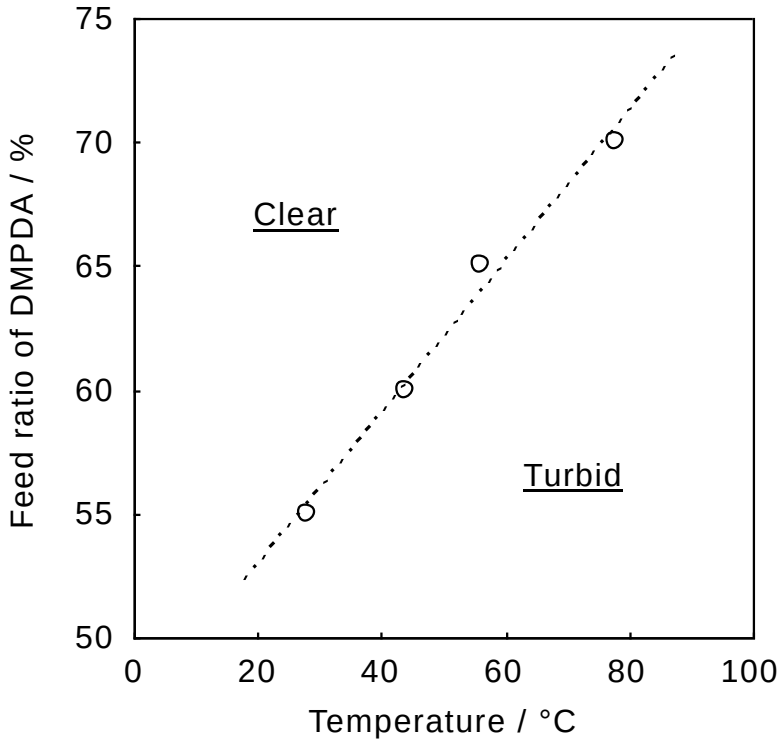

Fig. 5. Relationship between composition ratio of DMPDA and the LCST. The LCST was defined as 50 % transmittance. The measurements were performed at 500 nm at a heating rate of 1.0 ˚C/min.

content of DMPDA in the polymer (Fig. 5).

3.1.3. Particle size

Temperature dependence of the particle size of polymer **2d** in water, determined by DLS measurements, was shown in Fig. 6. At 10 ˚C, this temperature was lower than the sol−gel phase transition temperature (T_{sg}), the particle size was approximately 10−30 nm, and their distribution was not much broad. On the other hand, the particle size of the aggregates increased gradually and had a wide distribution with increasing temperature. At 30 ˚C in the gel state, the particle with a very broad distribution, from tens of nm to about 1000 nm, was observed. Soon thereafter this very broad distribution split into the large particle of about 1000 nm and the small particle of 60 nm at 35 ˚C. With further heating, small particles disappeared, and it was only large particles.

This change in particle size corresponds well with the change in physical properties of the polymer **2d**. PAD molecules form a micelle-like small aggregation in water below T_{sg}. This small aggregation assembled and become larger with increasing temperature. Then, large particles associate with each other, and the larger particles are formed. At this time, the polymer network including water molecules forms a hydrogel. Meanwhile, the light is scattered by the appearance of the submicron particles. As a result, the LCST phenomenon is caused.

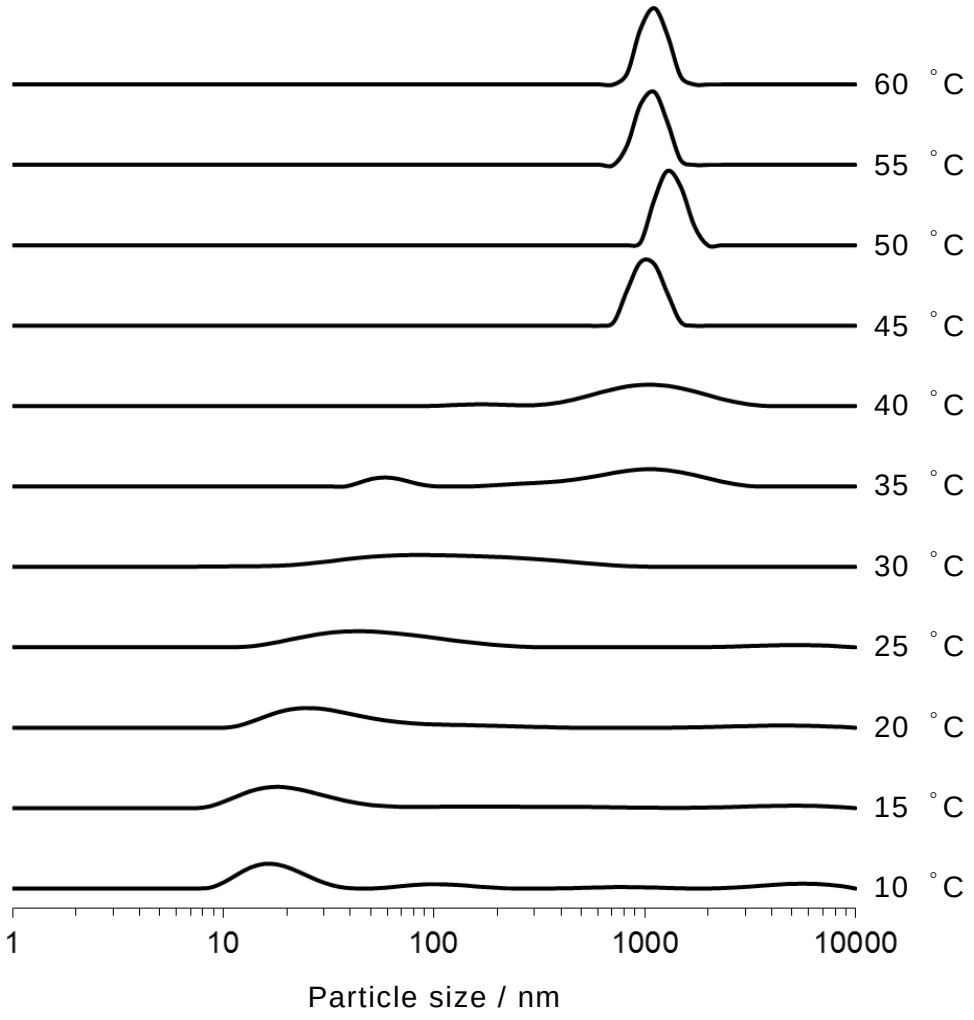

Fig. 6. Temperature dependence of particle size of polymer **2d** in 1.0 wt% aqueous solution.

3.1.4. TEM images

Fig. 7 shows TEM pictures of 0.01 wt% aqueous solution of polymer **2d**. At 25 ˚C in the gel state, particles with various size and shape were densely packed across the field of view (Fig. 7(A)), and the spherical aggregate about 1000 nm was observed at 45 ˚C above the LCST (Fig. 7(B)). These facts are direct evidence that polymer network formed by the particles is responsible for the physical gelation and the formation of aggregates cause turbidity phenomenon.

3.2. Thermo-responsive PAD using AP as hydrophilic group

3.2.1. Physical properties

Fig. 8 depicts the temperature dependence of the viscosity of 10 wt% aqueous solutions of polymers **3a−d** on the heating process in the temperature range from 10 ˚C to 70 ˚C. As the LA content in polymers increased, the temperature of the maximum viscosity decreased and the maximum viscosity increased. These behaviors were similar to those of PAD using DMPDA. On the other hand, no thermo-responsibility was observed in sample **3d** containing the hydrophilic AP unit over 65 %.

Furthermore, the viscoelastic properties of 10 wt% solution of polymer **3b** were shown in Fig. 9. These behaviors were also similar to those of PAD using DMPDA. In the case of **3b**, The sol−gel phase transition occurs at 29 ˚C and the gel−sol phase transition occurs at 61 ˚C.

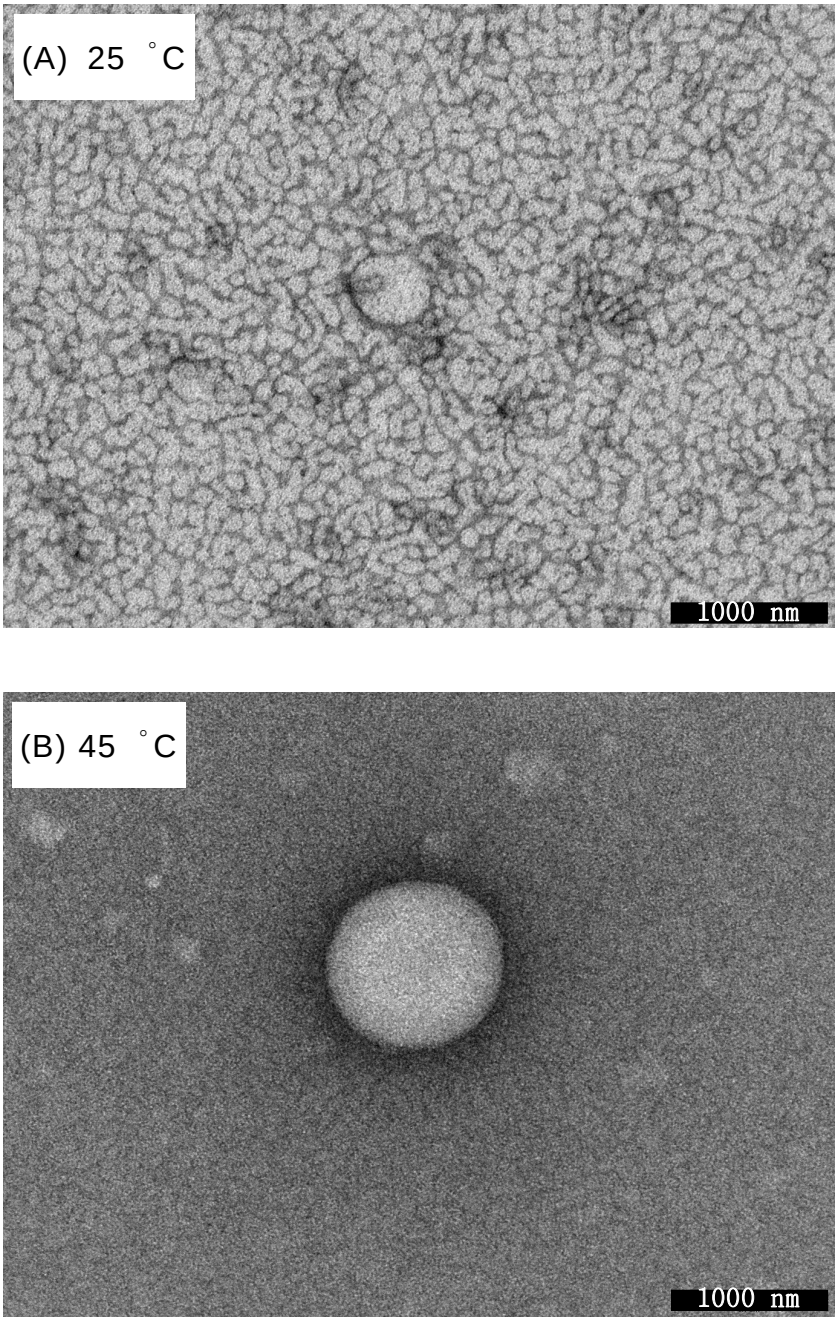

Fig. 7. TEM images of 0.01 wt% aqueous solution of polymer **2d** at (A) 25 °C and (B) 45 °C. Scale bar represents 1000 nm.

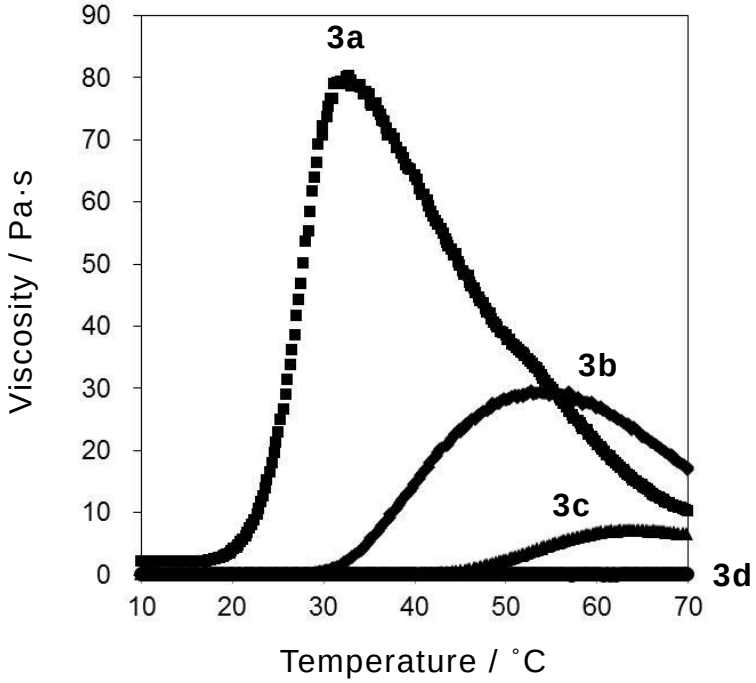

Fig. 8. Temperature dependence of apparent viscosity for 10 wt% PAD aqueous solutions (polymers **3a–3d**).

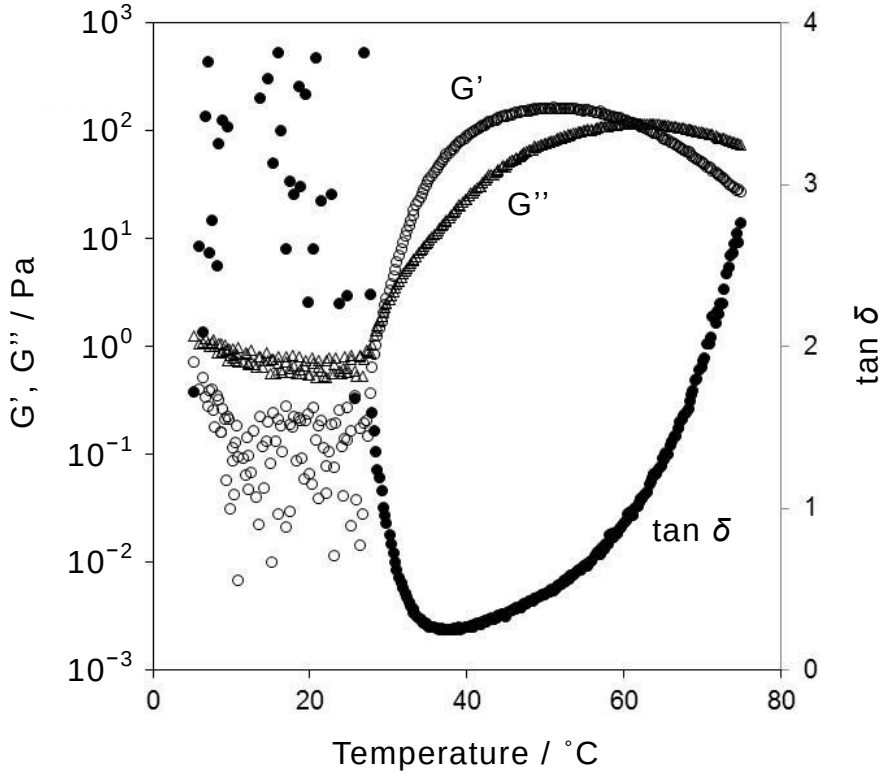

Fig. 9. Temperature dependence of storage modulus (G'), loss modulus (G'') and tan δ for 10 wt% polymer **3b** aqueous solution.

3.2.2. Phase separation behavior

However, the aqueous solution of PAD including AP unit does not show turbidity with heating. Consequently, PADs using AP (**3a−d**) has no LCST.

3.2.3. Particle size

Temperature dependence of the particle size of polymer **3b** in water, determined by DLS measurements, was shown in Fig. 10. Below the T_{sg}, particles with various sizes are mixed. On the other hand, particles larger than 1000 nm were extinguished at 30 ˚C in the gel state. With further heating, particles larger than 1000 nm again appeared over 50 ˚C. These behaviors are quite different from the PAD including DMPDA which physical properties are very similar.

3.2.4. TEM images

Fig. 11 shows TEM pictures of 0.01 wt% aqueous solution of polymer **3b**. At 20 ˚C in the sol state, particles with various size and shape dispersed (Fig. 11(A)). With increasing temperature, large particles disappeared, and PAD aqueous solution forms a uniform phase at 45 ˚C in the gel state (Fig. 11(B)). With further heating, particles appeared again at 70 ˚C. These TEM images are reproduced the results of the DLS measurements.

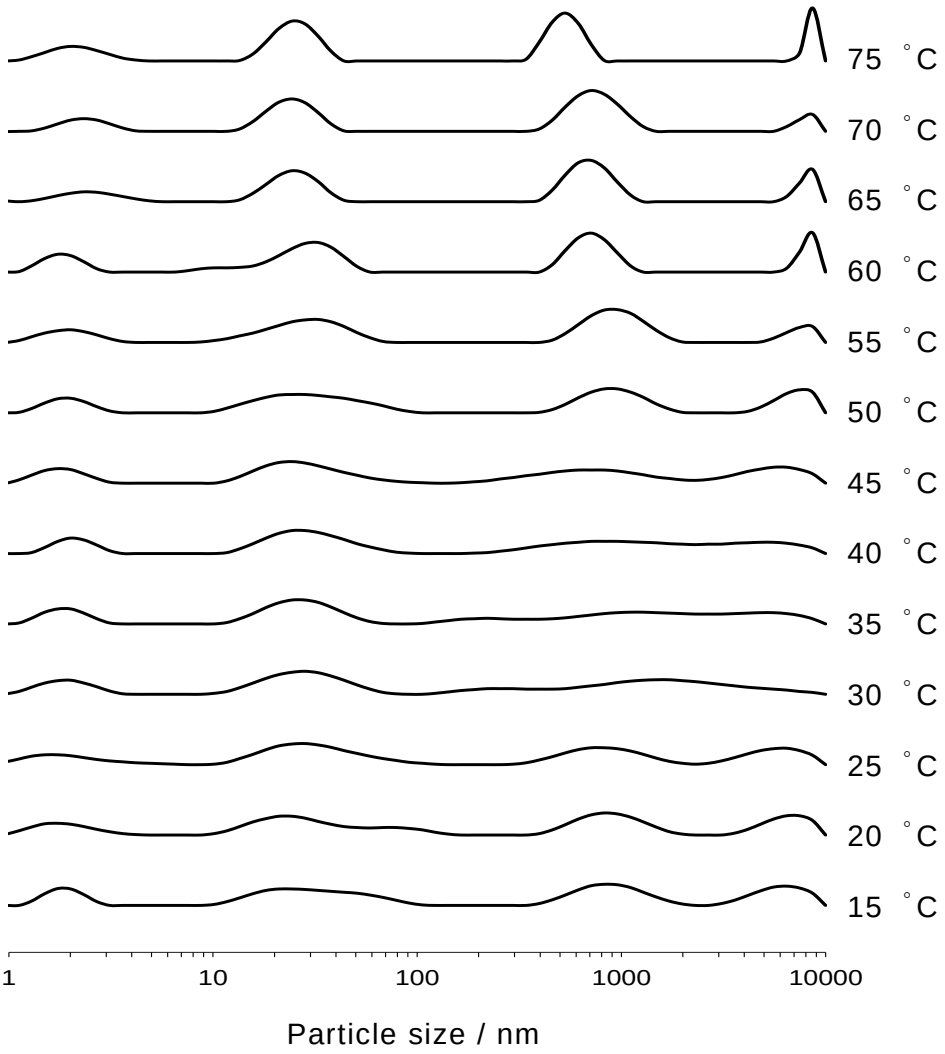

Fig. 10. Temperature dependence of particle size of polymer **3b** in 1.0 wt% aqueous solution.

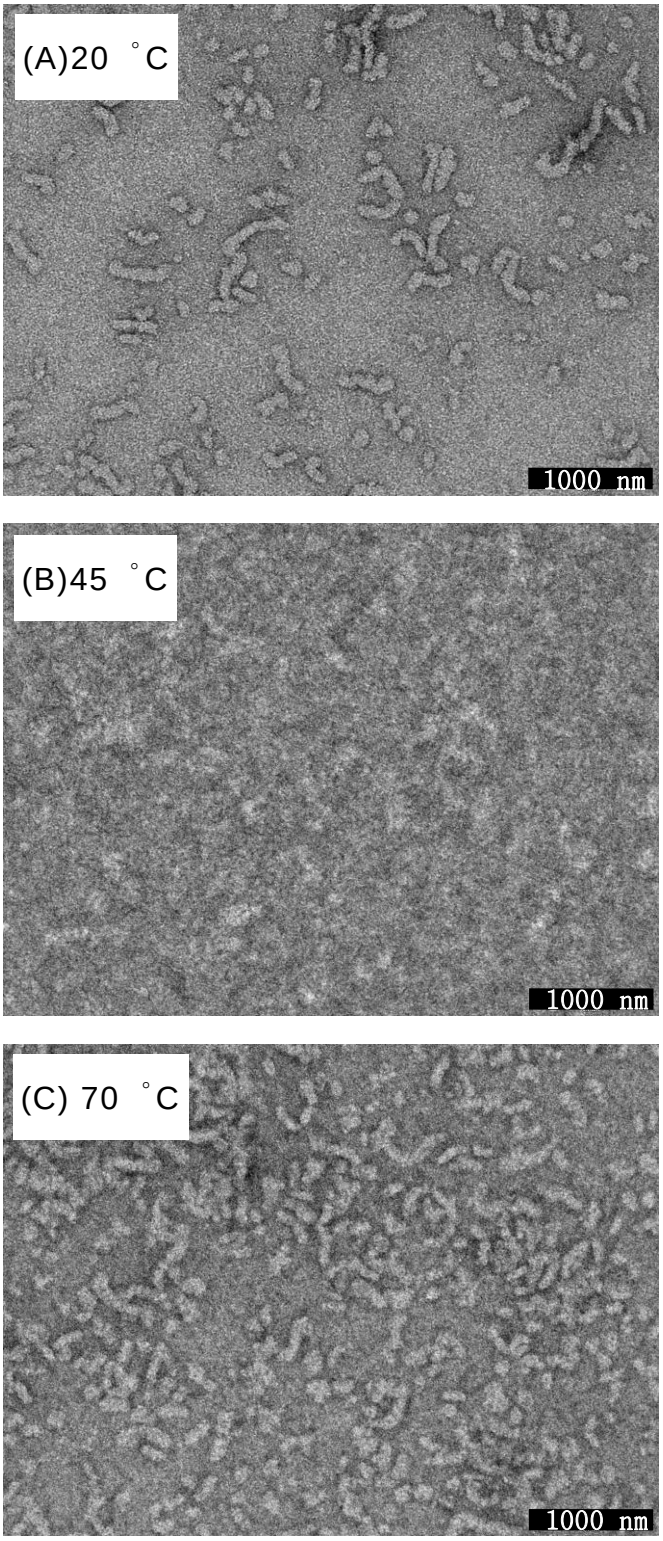

Fig. 11. TEM images of 0.01 wt% aqueous solution of polymer **3b** at (A) 20 °C, (B) 45 °C, and (C) 70 °C. Scale bar represents 1000 nm.

4. Conclusions

New thermo-responsive and biodegradable poly(asparagine) derivatives which show not only the LCST but also a sol−gel−sol phase transition were developed. These thermo-responsive properties could be precisely controlled by changing the composition of the side chain in PAD. The present unique sol−gel−sol phase transition and the LCST of PAD have great potential for various applications.

In addition, these characteristic phenomena of phase separation and gelation with increasing temperature were confirmed by DLS measurements and TEM images. In the case of PAD with DMPDA, the micelle-like small aggregates at low temperature are assembling, and the larger aggregates were formed with heating. The driving force of thermo-responsiveness in this DMPDA case is described by a conventional model which has been proposed. However, the thermo-gelation mechanism of the PAD with AP as a hydrophilic group in water was quite different from that with DMPDA.

References

[1] M. Heskins, J. E. Guillet, *J. Macromol. Sci. Chem.*, A2 (1968) 11441.

[2] G. Chen, A. S. Hoffman, *Nature*, 373 (1995) 49.

[3] B. Jeong, S. W. Kim, Y. H. Bae, *Adv. Drug Delivery Rev.*, 54 (2002) 37.

[4] T. G. Park, A. S. Hoffman, *J. Biomed. Mater. Res.*, 21 (1990) 24.

[5] H. Uyama, S. Kobayashi, *Chem. Lett.*, (1992) 1643.

[6] H. Çicek, T. Tuncel, *J. Polym. Sci., Polym. Chem. Ed.*, 36 (1998) 543.

[7] M. Kurisawa, Y. Matsuno, N. Yui, *Macromol. Chem. Phys.*, 199 (1998) 705.

[8] C. Ramkissoon-Ganorkar, F. Liu, M. Baudys, S. W. Kim, *J. Controlled Release*, 59 (1999) 287.

[9] M. Kurisawa, Y. Yokoyama, T. Okano, *J. Controlled Release*, 68 (2000) 1.

[10] A. Tuncel, E. Ünsal, H. Çicek, *J. Appl. Polym. Sci.*, 77 (2000) 3154.

[11] B. Jeong, Y. H. Bae, D. S. Lee, S. W. Kim, *Nature*, 388 (1997) 860.

[12] M. Malmsten, B. Lindman, *Macromolecules*, 25 (1992) 5440.

[13] T. Yoshida, K. Seno, S. Kanaoka, S. Aoshima, *J. Polym. Sci., Part A: Polym. Chem.*, 43 (2005) 1155.

[14] M. Obst, A. Steinbüchel, *Biomacromol.*, 5 (2004) 1166.

[15] Y. Tachibana, M. Kurisawa, H. Uyama, S. Kobayashi, *Biomacromol.*, 4 (2003) 1132.

[16] Y. Tachibana, M. Kurisawa, H. Uyama, T. Kakuchi, S. Kobayashi, *Chem. Lett.*, 32 (2003) 374.

[17] Y. Tachibana, M. Kurisawa, H. Uyama, T. Kakuchi, S. Kobayashi, *Chem. Commun.*, (2003) 106.

[18] H. S. Kang, S. R. Yang, J.-D. Kim, S.-H. Han, I.-S. Chang, *Langmuir*, 17 (2001) 7501.

[19] S. Sugihara, K. Hashimoto, S. Okabe, M. Shibayama, S. Kanaoka, S. Aoshima, *Macromolecules*, 37 (2004) 336.

[20] C. T. Huynh, M. K. Nguyen, D. S. Lee, *Macromolecules*, 44 (2011) 6629.

Chapter 3

Characterization of Thermo-responsive Poly(asparagine) Derivative in DMSO/Water System by Solution NMR

1. Introduction

There has been great interest in polymers exhibiting the phase transition that is readily reversible with thermal stimulus. Thermo-responsive polymers have been widely investigated for various applications such as controlled drug delivery, biomedical materials, fillers of column chromatography, gene-transfection agents, immobilized biocatalysts, and others [1−8]. Poly(*N*-isopropylacrylamide) (PNIPAM) is currently the most extensively studied thermo-responsive polymer. PNIPAM exhibits a rapid and reversible hydration−dehydration change in response to small temperature cycles around its lower critical solution temperature (LCST) [9−11]. In addition to PNIPAM and NIPAM-containing copolymers, various thermo-responsive polymers, typically poly(vinyl methyl ether), poly(2-isopropyl-2-oxazoline), poly(N-vinylalkylamide)s, and poly(phosphazene)s, have been developed [12−15]. However, non-biodegradability of these polymers may restrict their applications in the biomedical field.

Polypeptides and related artificial poly(amino acid)s have become

important materials because of their specific properties of biodegradability, biocompatibility, and others [16]. Poly(*α*/*β*-aspartic acid), which is synthesized by thermal polymerization of aspartic acid, followed by alkaline hydrolysis, is expected to be an alternative to non-biodegradable poly(acrylic acid) widely used in various industrial fields. Recently, it was reported that the poly(aspartic acid) derivatives formed a micelle in an aqueous solution, and new thermo-responsive polymers based on biodegradable poly(amino acid)s, poly(*N*-substituted *α*/*β*-asparagine)s, which had a LCST and showed a sol−gel−sol phase transition in water, have been developed [17−22].

This chapter deals with a biodegradable and thermo-responsive amphiphilic poly(*N*-substituted *α*/*β*-asparagine) derivative (PAD) showing a sol−gel−sol phase transition behavior. Especially, the detailed structural characterization of this polymer with the hydroxyl group in the terminal moieties of the hydrophilic side chains in water was investigated using ^{13}C solution NMR spectroscopy. After the isolated PAD structure was assigned in DMSO, the structural feature of thermo-responsive PAD in water was revealed by addition of D_2O gradually to DMSO solution.

2. Experimental section

*2.1. Preparation of thermo-responsive PAD (**2**)*

Poly(succinimide) (**1**) prepared by thermal polycondensation with M_w and M_w/M_n of 9.8 x 10^4 and 1.45, respectively, was used as a precursor. The M_w and M_w/M_n of **1** was determined by gel permeation chromatography (GPC) analysis eluted by *N*,*N*-dimethylformamide (DMF) containing 0.1M LiBr with KD-804 (Shodex) column. Thermo-responsive PAD (**2**) was prepared from **1** with a mixture of laurylamine (LA) and 3-amino-1-propanol (AP) in DMF (Scheme 1) [21,22]. The feed ratio of each amine was LA : AP = 20 : 80. In addition, purification to remove the residual aminium salts was also performed by using an ion exchange resin.

2.2. Measurements

The dynamic viscosity of the 10 wt% PAD aqueous solution was measured using a stress-control-type rheometer (Viscoanalyzer Var-50/100, Reologica Instrument, AB) equipped with a parallel plate geometry (40 mm diameter) at a heating ratio of 1.0 ˚C/min at a constant frequency (1.0 Hz). The temperature was controlled within 0.1 ˚C by a Peltier element.

2.3. NMR spectroscopy

All NMR spectra were obtained using a Bruker AVANCE III 500

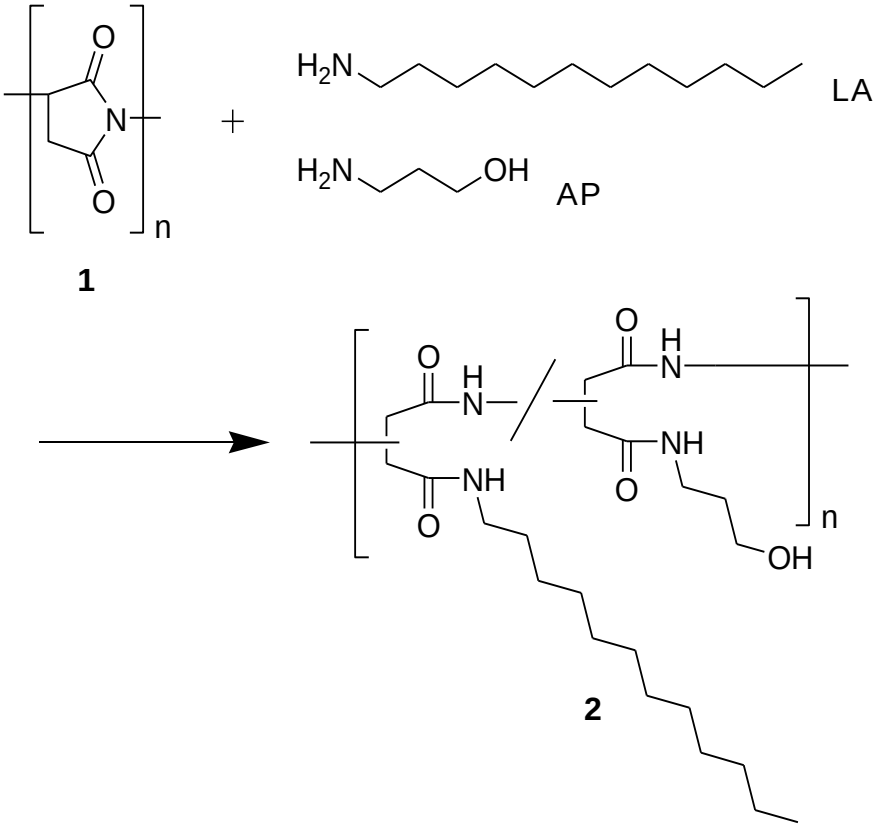

Scheme 1. Synthetic scheme showing the preparation of poly(*N*-substituted *α*/*β*-asparagine) derivative (PAD).

spectrometer operating at 500 MHz for the 1H nucleus and 125 MHz for the ^{13}C nucleus. Sample solutions for NMR were prepared by dissolving 60 mg of polymer in 0.6 mL of each solvent in 5 mm NMR tubes. All spectra were recorded at 25 ˚C. The conditions for ^{1}H NMR were a 30 ˚ pulse angle, a 4.17 s delay between pulses, a 10.3 kHz spectral width, 32K data points, and 4 scans. The conditions for ^{13}C NMR were a 45 ˚ pulse angle, a 5.5 s delay between pulses, a 29.7 kHz spectral width, 64 K data points, and 2048 scans. The DEPT135 spectrum was collected with a 0.9 s recovery delay, a 31.2 kHz spectral width, 64 K data points, 10.0 μs 90 ˚ ^{13}C pulses, and 128 scans. The COSY spectrum was acquired in the magnitude mode using 1 scan for each of the 128 t1 increments, a 1.97 s recovery delay, spectral widths in f1 and f2 of 5.8 kHz, an acquisition time of 0.176 s, and 10.0 μs 90 ˚ ^{1}H pulses. Data were processed with sine bell weightings and zero-filled to a 1K x 512 data matrix. The HSQC spectrum was acquired in the phase sensitive mode using 8 scans for each of the 256 t1 increments, a 1.5 s recovery delay, spectral widths in f1 and f2 of 8.8 and 5.0 kHz, respectively, an evolution delay (1/(2J)) of 3.45 ms, an acquisition time of 0.102 s, 10.0 μs 90 ˚ ^{1}H pulses, and 10.0 μs 90 ˚ ^{13}C pulses. Data were processed with squared sine bell weightings and zero-filled to a 1K x 1K data matrix.

3. Results and Discussion

3.1. Physical properties

The sol−gel−sol phase transition of **2** in water was confirmed by viscosity measurement in the temperature range from 20 ˚C to 70 ˚C. The aqueous solution of PAD showed a significant increase in viscosity around 40 ˚C. The solution concentration produced great effect on the viscosity of this polymer solution. The maximum viscosity of 10 wt% polymer solution was approximately 70 Pa·s observed at 58 ˚C. With further heating, the viscosity of PAD aqueous solution decreased gradually.

3.2. Assignment of ^{1}H and ^{13}C NMR spectra of the thermo-responsive PAD

Dimethyl sulfoxide (DMSO) is a good solvent for **2**, and this thermo-responsive PAD does not show the unique properties in DMSO different from in water. First of all, the structural analysis of synthesized polymer was carried out in deuterated DMSO (DMSO-d_6) using the NMR techniques to keep the uncondensed structural information in detail. The ^{1}H and ^{13}C NMR spectra of **2** in the DMSO-d_6 are shown in Figs. 1 and 2, respectively. The assignments of the signals were obtained for the most part by a combination of the following: (1) analysis of the proton−proton and proton−carbon connectivity in the two-dimensional (2D) NMR spectra; (2) distinction of the methine, methylene, and methyl carbon using DEPT135 spectrum; (3) internal consistency in the ^{1}H and ^{13}C NMR signal areas and

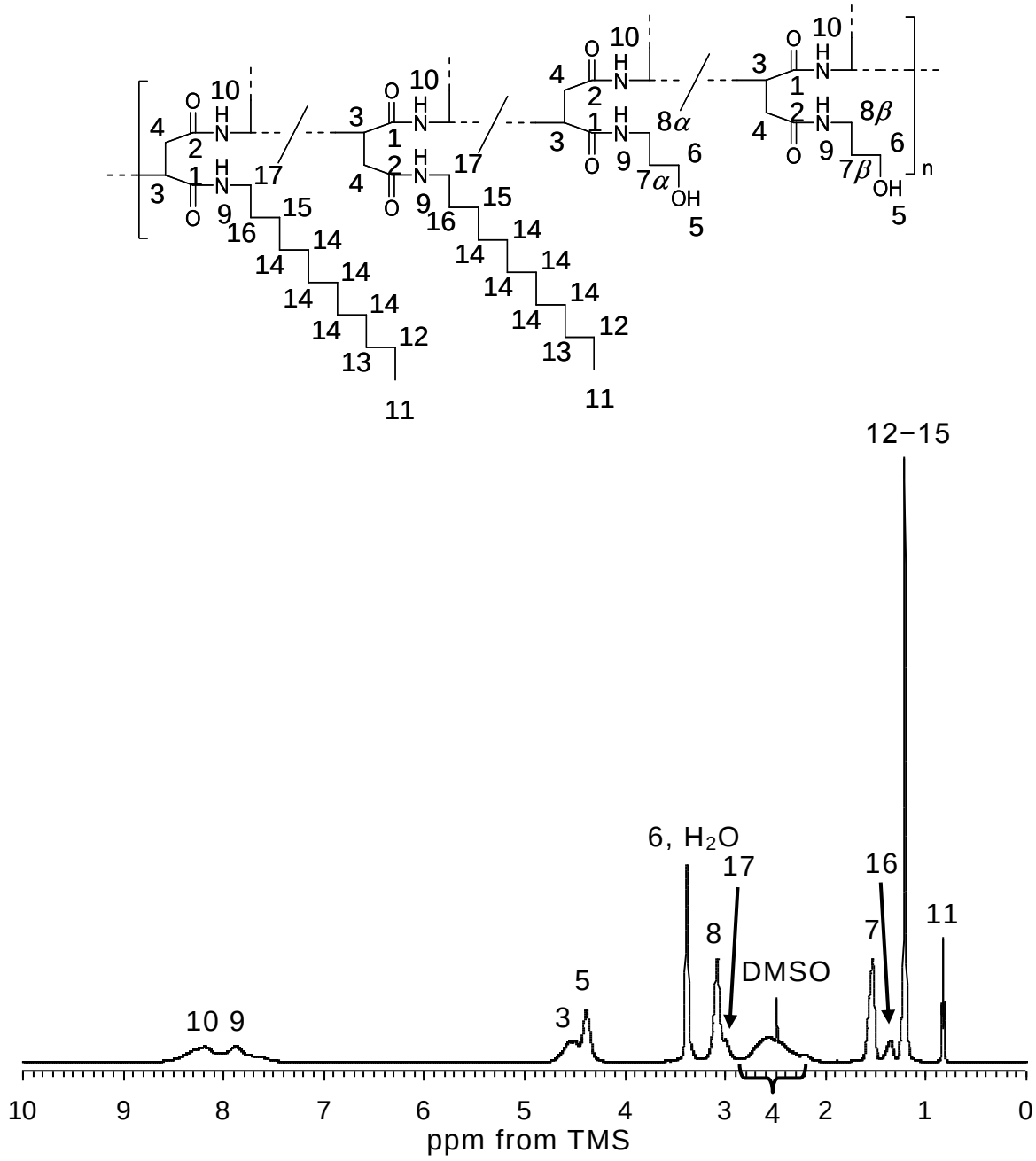

Fig 1. ^{1}H NMR spectrum of PAD sample **2** in DMSO-d_6 (10 wt%).

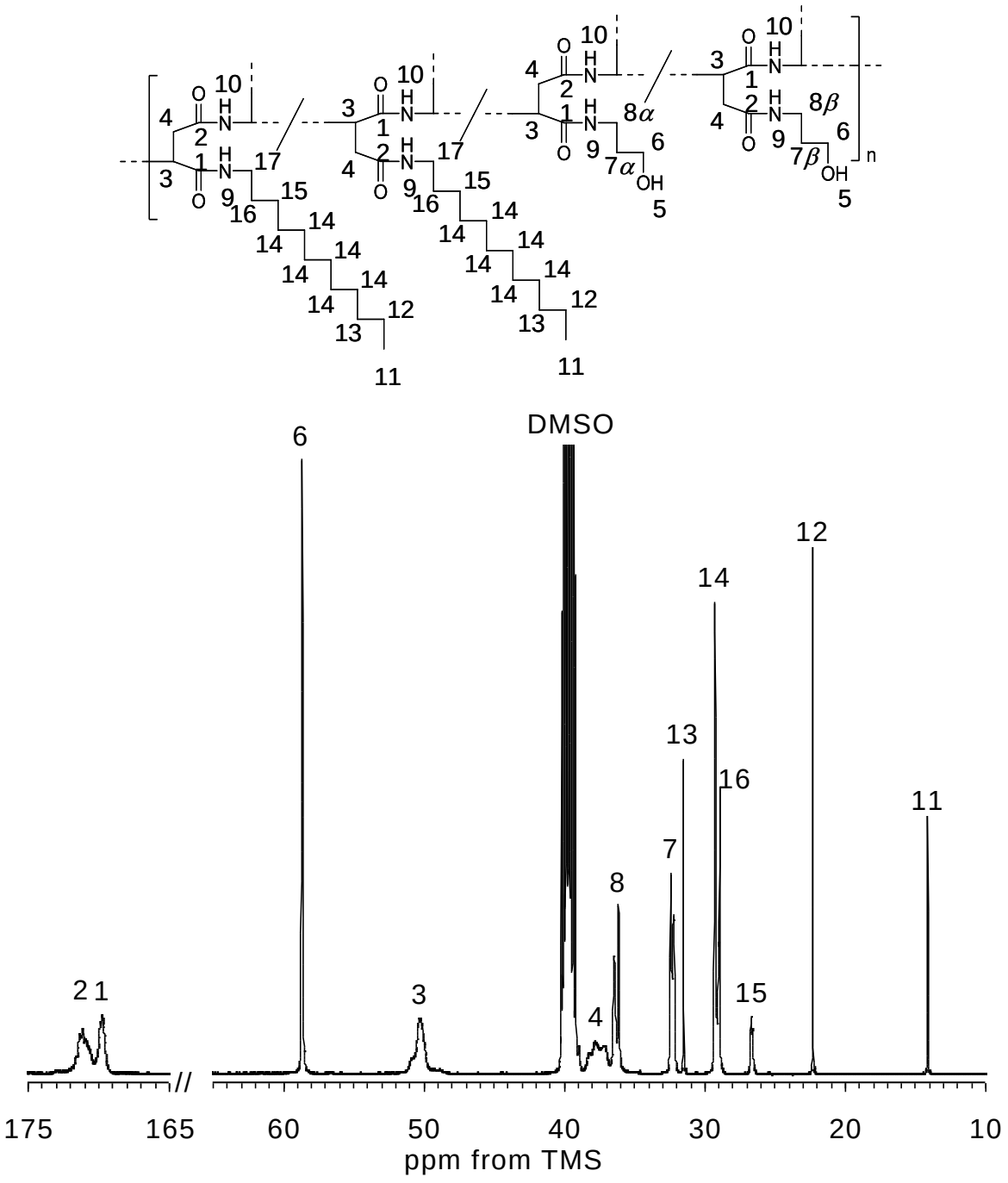

Fig 2. ^{13}C NMR spectrum of PAD sample **2** in DMSO-d_6 (10 wt%). The numbers in the spectrum correspond to those in Figure 1.

quantitative consistency between the ^{1}H and ^{13}C NMR signal areas; (4) changes in the chemical shifts with the gradual addition of D_2O.

It must be mentioned that the signal at 47.4 ppm disappeared completely, suggesting that all of the succinimide units have been converted into the *N*-substituted *α*/*β*-amide unit. The two kinds of carbonyl carbons adjacent to the methine and methylene carbons were assigned to the peaks at 169.8 and 171.2 ppm, respectively, referred to the 2D-INADEQUATE spectrum [23]. The broad signal at 50.3 ppm was correlated to the methine carbon C-3 in the main chain in the DEPT135 spectrum [24], and another broad signal around 37.0−38.5 ppm was assigned to the methylene carbon C-4 in the main chain. The protons around 4.30−4.70 ppm (H-3) and 2.20−2.80 ppm (H-4) were directly attached to the C-3 and C-4, respectively, in the HSQC spectrum shown in Fig. 3. Based on the corresponding chemical shift, the signal at 58.6 ppm was assigned to the methylene carbon C-5 adjacent to the hydroxyl group in the hydrophilic side chain which was derived from AP. The protons at 3.38 ppm (H-5) were directly bonded to the C-5 (Fig. 3). This H-5 gave cross-peak to the signal at 1.53 ppm (H-7), then the H-7 also gave cross-peak to the signal at 3.08 ppm (H-8), and finally the H-8 was linked to the proton of the amide group (H-9) in Fig. 4. Meanwhile, the carbons which were directly attached to the H-7 and H-8 were assigned in the HSQC spectrum (Fig. 3). The signals at 7.89 ppm (H-9) and 8.20 ppm (H-10) were assigned to the protons derived from the amide group in the side chain (directly attached to the methylene carbon) and in the main chain (directly attached to the methine carbon), respectively, in Fig. 4. In the same way as the assignment of the side chain from AP, the long alkyl hydrophobic side chain

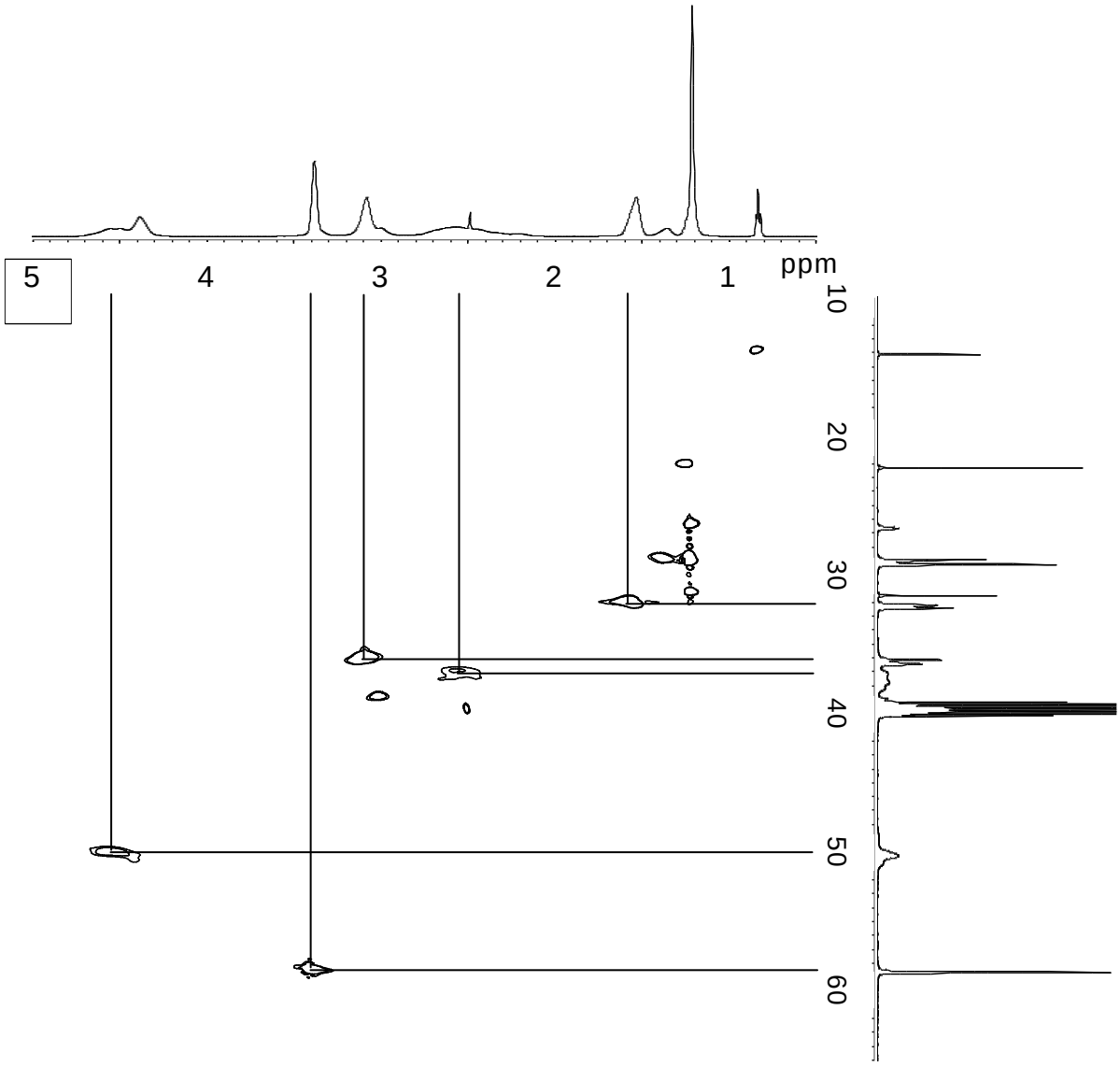

Fig 3. H−C HSQC spectrum of PAD sample **2** in DMSO-d_6, expanded methyl and methylene region.

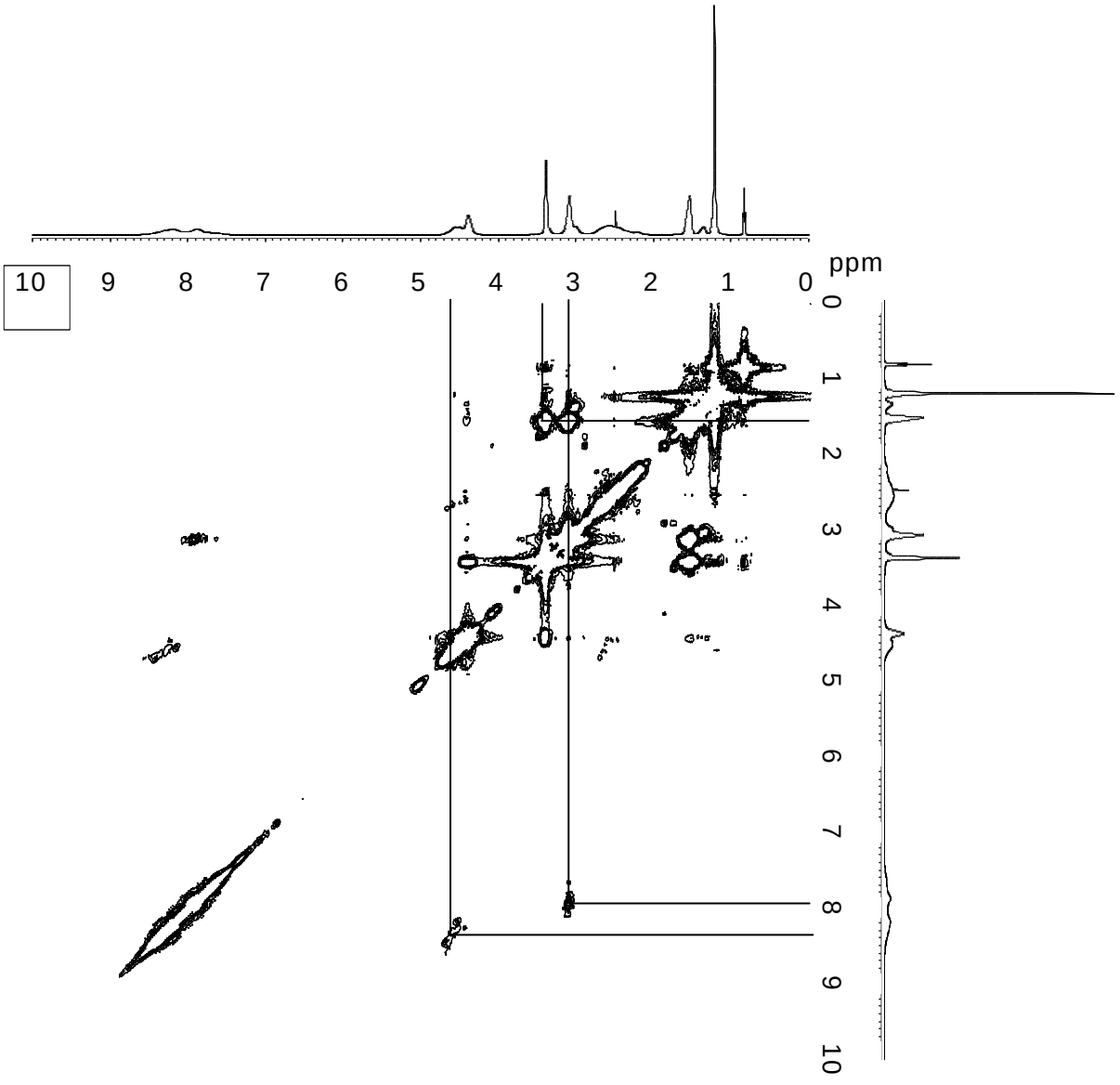

Fig 4. H−H COSY spectrum of PAD sample **2** in DMSO-d_6.

derived from LA could be also assigned from the terminal methyl carbon at 14.1 ppm (C-11) and proton at 0.83 ppm (H-11). However, the signal of the methylene carbon (C-17) adjacent to the amide group was not observed because of the overlapping with the signal derived from the DMSO-d_6.

3.3. The primary structure of thermo-responsive PAD in water

The primary structure of the thermo-responsive PAD (**2**) in water was revealed by tracking changes in the chemical shifts with gradually-added D_2O to the DMSO-d_6 solution of **2**. As a reference for the chemical shift and peak intensity 1,4-dioxane was used. Fig. 5 showed the ^{13}C NMR spectra of 10 wt% solution of **2** with changing the ratio between DMSO-d_6 and D_2O.

The intensity of all signals originated from thermo-responsive PAD (**2**) was reduced with increasing the ratio of D_2O. The signals of C-4 in main chain and C-17 in hydrophobic LA chain were impossible to observe during these measurements because of overlapping with DMSO. Such decline of intensity indicates a decrease in the mobility of polymer chain in water compared with that in DMSO. The reduction degree of signal intensity of hydrophobic side chain from LA was significant than that of hydrophilic side chain from AP. Namely, the mobility of LA side chain was restricted than that of AP side chain in water.

On the other hand, the detailed partial structure of thermo-responsive PAD (**2**) in water was revealed by the chemical shift values of corresponding signals. Fig. 6 showed the changes in chemical shifts of hydrophilic AP side chain and hydrophobic LA side chain upon addition of D_2O to the DMSO-d_6.

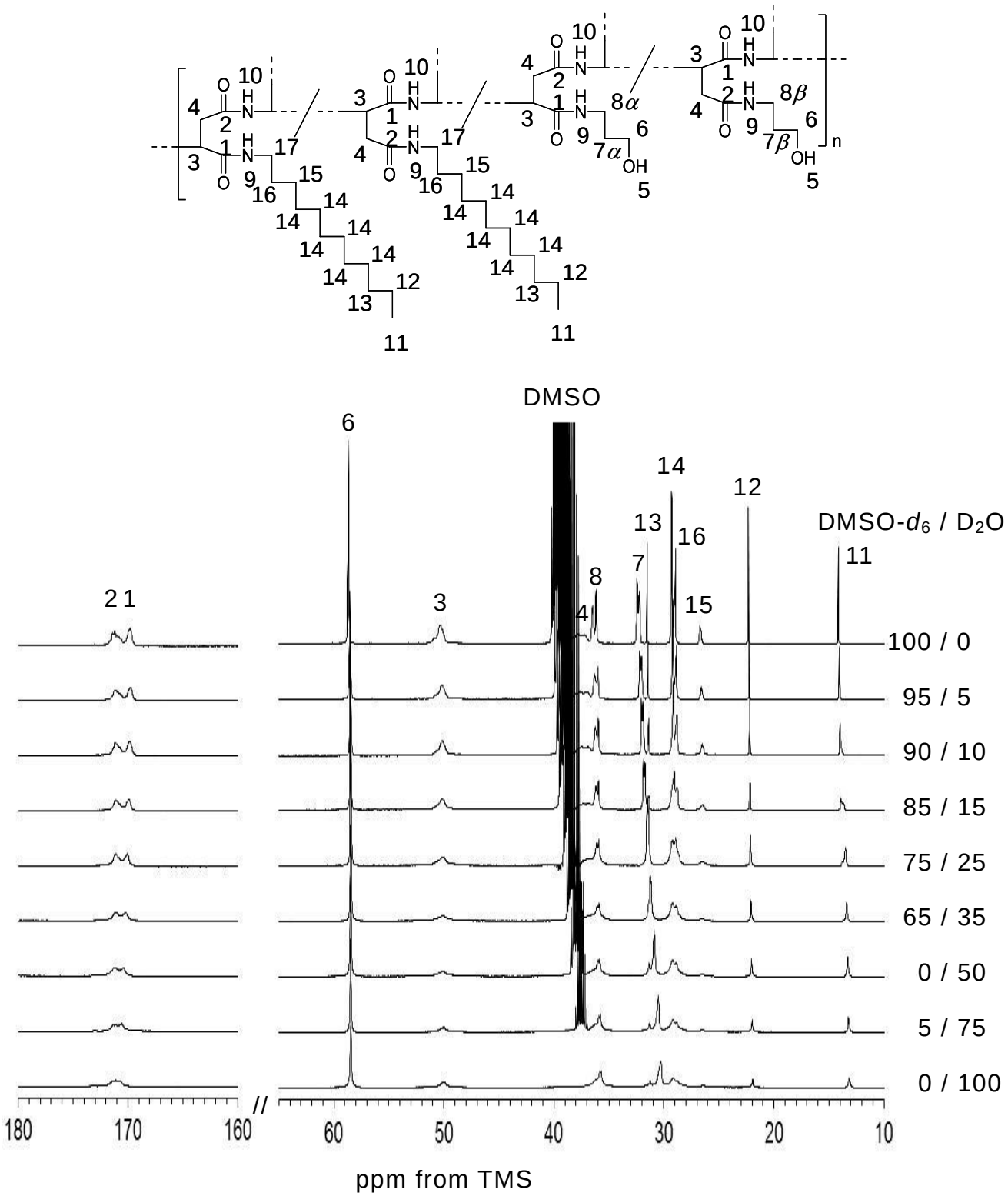

Fig 5. ^{13}C NMR spectra of PAD sample **2** as a function of the DMSO-d_6 and D_2O ratio.

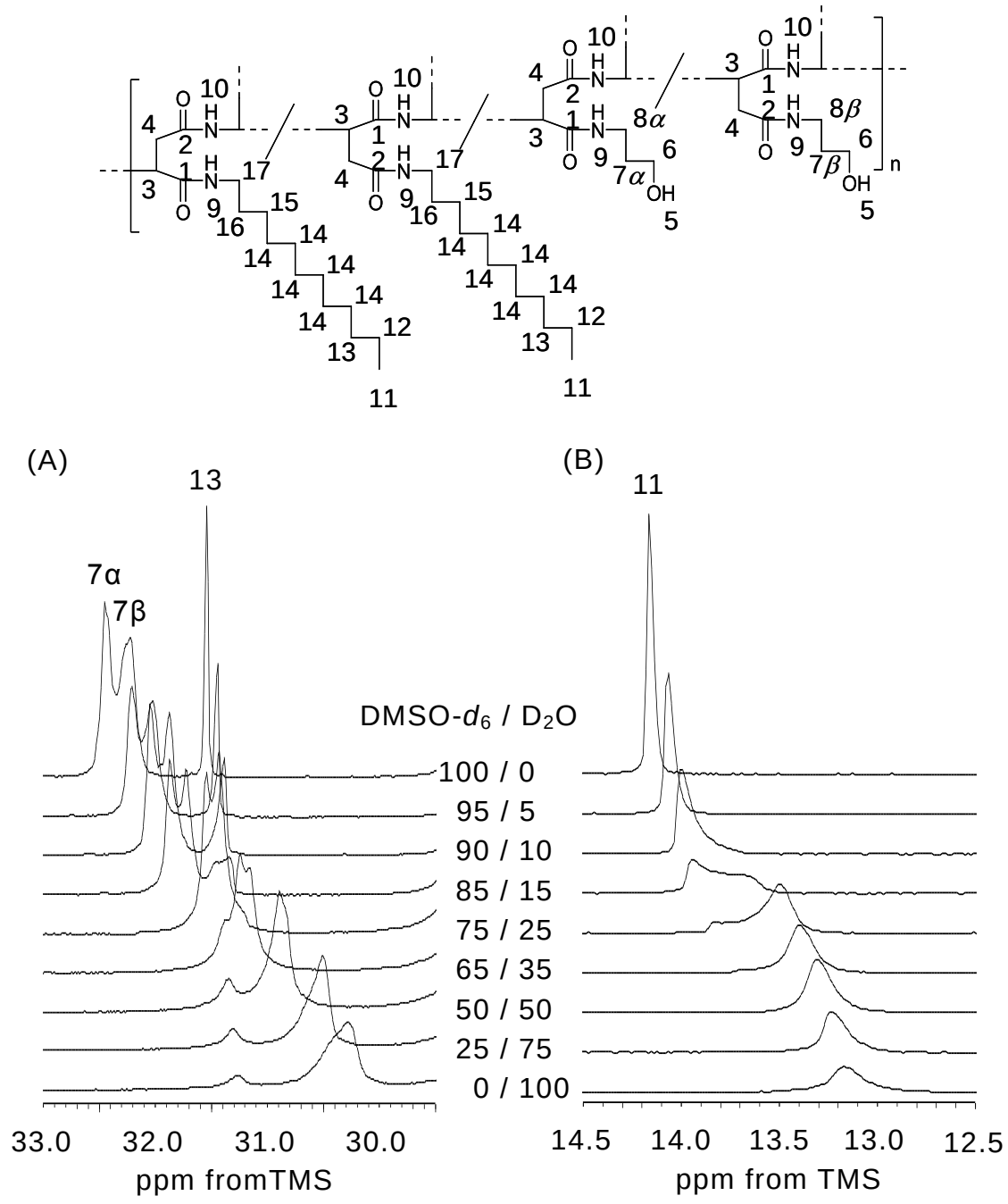

Fig. 6. Expanded PAD ^{13}C NMR spectra as a function of the DMSO-d_6 and D_2O ratio; (A) central methylene carbon region of the AP side chain, (B) terminal methyl carbon region of the LA side chain.

The central methylene group in the AP unit (C-7) was upfield shifted gradually with increasing the D_2O content, and the amount of the C-7 upfield shift was also approximately 2.0 ppm (Fig. 6(A)). The amount of the terminal methyl group in the LA unit (C-11) upfield shift was approximately 1.0 ppm, and this shift was observed at the 15−25 % D_2O ratio in Fig. 6(B). Other carbons derived from AP and LA were little changed with addition of water. These upfield shifts are due to the γ-gauche effect in the ^{13}C chemical shift [25]. In brief, with addition of D_2O, C-7 from AP side chain shrank gradually and continuous, but C-11 from LA side chain abruptly shrank at the 15−25 % D_2O content. More specifically the central part in the AP side chain and the terminal part in the LA side chain appeared to change local conformation from all-trans to partial-gauche conformation in aqueous solution.

4. Conclusions

The thermo-responsive PAD (**2**) aqueous solution formed a hydrogel without any additives. Materials, which consist of the poly(amino acid) derivative and indicate the thermo-responsive property, are expected to be applicable for injectable biomedical device, controlled release of drugs, tissue engineering, and others.

This PAD in aqueous solution was characterized by using NMR techniques. The mobility of PAD molecules was reduced in water. In particular, the hydrophobic segment was extremely restricted as compared to the hydrophilic segment by strong hydrophobic interaction. At this time, a part of side chains derived from AP and LA was changed from extended state to contracted state. Namely, this amphiphilic PAD forms a micelle like aggregation structure under water.

References

[1] T. G. Park, A. S. Hoffman, *J. Biomed. Mater. Res.*, 24 (1990) 21.

[2] H. Uyama, S. Kobayashi, *Chem. Lett.*, (1992) 1643.

[3] M. Kurisawa, Y. Matsuno, N. Yui, *Macromol. Chem. Phys.*, 199 (1998) 705.

[4] H. Çicek, T. Tuncel, *J. Polym. Sci. Part A: Polym. Chem.*, 36 (1998) 543.

[5] A. Kikuchi, M. Okuhara, F. Karikusa, Y. Sakurai, T. Okano, *J. Biomater. Sci. Polym. Ed.*, 9 (1998) 1331.

[6] C. Ramkissoon-Ganorkar, F. Liu, M. Baudyš, S. W. Kim, *J. Controlled Release*, 59 (1999) 287.

[7] M. Kurisawa, M. Yokoyama, T. Okano, *J. Controlled Release*, 68 (2000) 1.

[8] A. Tuncel, E. Ünsal, H. Çicek, *J. Appl. Polym. Sci.*, 77 (2000) 3154.

[9] M. Heskins, J. E. Guillet, *J. Macromol. Sci. Part A Pure and Appl. Chem.*, 2 (1968) 1441.

[10] G. Chen, A. S. Hoffman, *Nature*, 373 (1995) 49.

[11] B. Jeong, S. W. Kim, Y. H. Bae, *Adv. Drug Deliv. Rev.*, 54 (2002) 37.

[12] K. Suda, Y. Wada, Y. Kikunaga, K. Morishita, A. Kishida, M. Akashi, *J. Polym. Sci. Part A: Polym. Chem.*, 35 (1997) 1763.

[13] B. H. Lee, Y. M. Lee, Y. S. Sohn, S.-C. Song, *Macromolecules*, 35 (2002) 3876.

[14] Y. Chang, E. S. Powell, H. R. Allcock, S. M. Park, C. Kim, *Macromolecules*, 36 (2003) 2568.

[15] C. Diab, Y. Akiyama, K. Kataoka, F. M. Winnik, *Macromolecules*, 37 (2004) 2556.

[16] M. Obst, A. Steinbüchel, *Biomacromolecules*, 5 (2004) 1166.

[17] Y. Tachibana, M. Kurisawa, H. Uyama, S. Kobayashi, *Biomacromolecules*, 4 (2003) 1132.

[18] Y. Tachibana, M. Kurisawa, H. Uyama, T. Kakuchi, S. Kobayashi, *Chem. Lett.*, (2003) 374.

[19] Y. Tachibana, M. Kurisawa, H. Uyama, T. Kakuchi, S. Kobayashi, *Chem. Commun.*, (2003) 106.

[20] H. S. Kang, S. R. Yang, J.-D. Kim, S.-H. Han, I.-S. Chang, *Langmuir*, 17 (2001) 7501.

[21] E. Watanabe, N. Tomoshige, *Chem. Lett.*, (2005) 876.

[22] E. Watanabe, N. Tomoshige, H. Uyama, *Macromol. Symp.*, 249/250 (2007) 509.

[23] K. Matsubara, T. Nakato, M. Tomida, *Macromolecules*, 30 (1997) 2305.

[24] K. Matsubara, T. Nakato, M. Tomida, *Macromolecules*, 31 (1998) 1466.

[25] T. Asakura, M. Demura, Y. Nishiyama, *Macromolecules*, 24 (1991) 2334.

Chapter 4

NMR Studies on Thermo-responsive Behavior of Poly(asparagine) Derivative in Water

1. Introduction

Stimuli-responsive polymers are becoming increasingly attractive for biotechnology and pharmaceutical applications [1,2]. In particular there has been great interest in polymers exhibiting thermally reversible phase transitions. Poly(*N*-isopropylacrylamide) (PNIPAM) is one of the most extensively studied thermo-responsive polymers. PNIPAM exhibits rapid and reversible hydration−dehydration in response to small temperature cycles around its lower critical solution temperature (LCST) [3,4]. PNIPAM, NIPAM-containing copolymers, and PNIPAM-based cross-linked hydrogels have been widely used as matrices in a variety of applications such as in controlled drug delivery, biomedical materials, fillers for column chromatography, gene-transfection agents and as immobilized biocatalysts [5−8].

Thermo-responsive polymers based on biodegradable and biocompatible poly(amino acid)s, poly(*N*-substituted *α*/*β*-asparagine) derivatives (PADs) that show a clear LCST and a sol−gel−sol phase transition in an aqueous solution have been developed [9−13]. These poly(amino acid)s

are expected to have important applications in biomedical fields due to their thermo-responsiveness, biodegradability, and high biocompatibility [14,15]. Thus far, the compounds which have shown physical properties such as a phase transition have been characterized by NMR, size exclusion chromatography, light scattering, fluorescence spectroscopy, electron microscopy, small-angle X-ray scattering, and field-flow fractionation [16−24]. Among these techniques, NMR allows for observing physical characteristics without the requirement of special preparation of the samples. NMR has the additional advantage of simultaneous estimation of phase contents and dynamical properties (e.g., through relaxation times) at the same time scale. Therefore by using NMR techniques the dynamics, structures, and interactions of molecular and/or polymeric systems can be elucidated and the complex relationship between chemical structure and macroscopic behavior may be readily explored [25,26].

In this chapter, several NMR methods to study the complex aggregation and dissociation process resulting in the liquid to gel transition of thermo-responsive aqueous solution PAD molecules have been used. Both ^{13}C solution and solid state CP/MAS NMR approaches were used to study the structure and dynamics of PAD molecules that gives rise to the observed phase transition [27−29]. In addition, deuterium two-dimensional (2D) T_1−T_2 and T_2−T_2 relaxation spectroscopies [30−32], based on an inverse Laplace transform (ILT) [33], were used to monitor the distribution, dynamics, and exchange of water in the PAD−water mixture during the phase transition. The 2D T_1−T_2 relaxation approach has been previously used to study the dynamics and distribution of water molecules in numerous multi-compartment systems.

For example, the technique was used to study the dynamical distribution of water in saturated sedimentary rock, processed starch and potato tissue, a variety of food products such as cheese and yogurt, cement paste and to probe the behavior of water in mechanically strained elastin [34−40]. This relatively new experimental technique correlates the measured T_1 and T_2 relaxation times in a 2D map, analogous to chemical shift correlation methods (such as COSY) that are based on Fourier transformation. In the T_2−T_2 approach one makes use of two consecutive measurements of T_2 relaxation times separated by an experimentally variable delay to probe exchange between reservoirs. The resulting 2D ILT may feature cross peaks indicating exchange between sites characterized by different T_2 relaxation times. Combined with ^{13}C NMR spectroscopy, the use of the T_1−T_2 and T_2−T_2 2D schemes in this work have allowed for a direct measure of water dynamics in the aqueous solution PAD and added insight into the liquid to gel phase transition.

2. Experimental section

*2.1. Preparation of thermo-responsive PAD (**2**)*

Poly(succinimide) (**1**) prepared by thermal polycondensation with M_w and M_w/M_n of 9.8×10^4 and 1.45, respectively, was used as a precursor. The M_w and M_w/M_n of **1** was determined by size exclusion chromatography (SEC) analysis eluted by *N*,*N*-dimethylformamide (DMF) containing 0.1 M LiBr with KD-804 (Shodex) column. Thermo-responsive PAD (**2**) was prepared from **1** with a mixture of laurylamine (LA) and 3-amino-1-propanol (AP) in DMF (Scheme 1) [11,13]. The quantitative introduction of the amine moiety was achieved by the addition of a mixture of the hydrophobic and the hydrophilic amines for PSI (**1**). In addition, purification to remove the residual amines was also performed by using an ion exchange resin.

2.2. Physical properties

The dynamic viscosity of the PAD aqueous solutions was measured using a stress-control rheometer (Viscoanalyzer Var-50/100, Reologica Instrument, AB) equipped with a parallel plate geometry (40 mm diameter) at a heating ratio of 2.0 ˚C/min at a constant frequency (1.0 Hz). The temperature in all viscosity measurements was controlled to within 0.1 ˚C by a Peltier element.

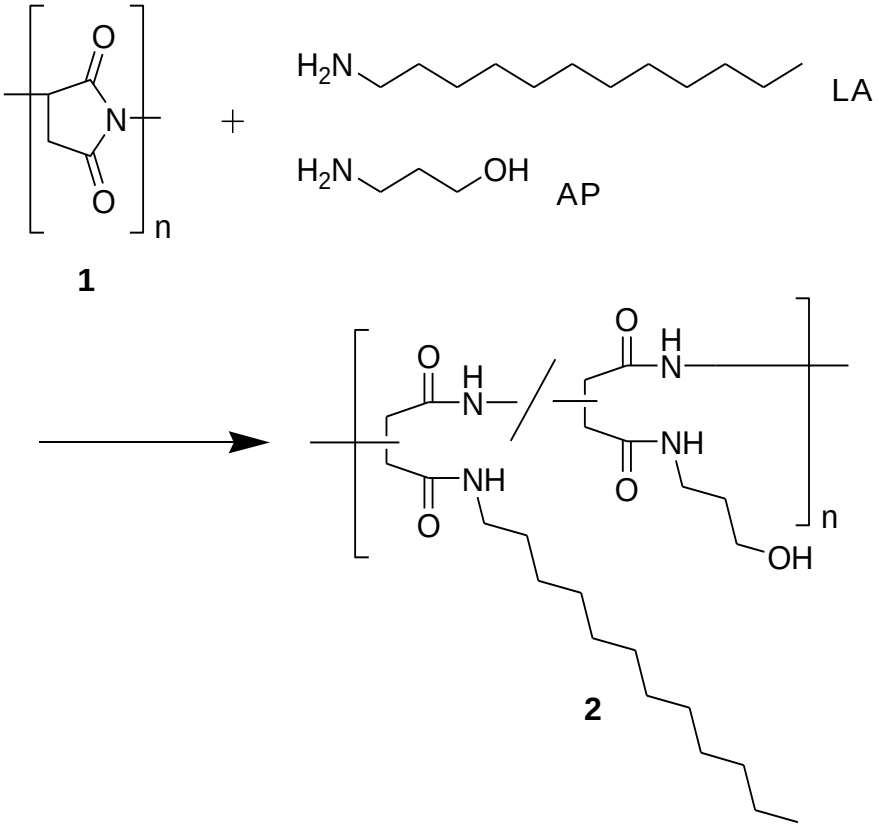

Scheme 1. Synthetic scheme showing the preparation of poly(*N*-substituted *α*/*β*-asparagine) derivative (PAD).

2.3. ^{13}C solution NMR spectroscopy

^{13}C solution NMR spectra were obtained by using a Bruker AVANCE III 500 spectrometer operating at 125 MHz for the ^{13}C nucleus at 25 ˚C. Deuterated water (D_2O) was used as solvents at a PAD sample concentration of 10 wt%. The chemical shift was adjusted to the 1,4-dioxane methylene peak observed at 65.9 ppm for ^{13}C NMR relative to tetramethylsilane at 0 ppm as an external standard. The conditions for ^{13}C NMR were a 45 ˚ pulse angle, a 5.5 s delay between pulses, a 29.7 kHz spectral width, 65536 data points, and 2048 scans.

2.4. ^{13}C CP/MAS NMR spectroscopy

^{13}C CP/MAS NMR spectra were recorded on a Chemagnetics CMX300 spectrometer operating at 75.6 MHz for ^{13}C observation. These measurements were carried out on a 10 wt% D_2O solution of sample **2-B** at 25, 40, 50, 60, and 70 ˚C. The temperature was calibrated by using $Pb(NO_3)_2$ based on previous literature [41]. The sample was contained in a cylindrical rotor made of zirconia and spun at 3 kHz. For cross polarization, the contact time was set to 3 ms and the pulse sequence recycle time was 5 s. The ^{13}C 90 ˚ pulse length was approximately 5.5 ms. The ^{13}C NMR chemical shifts were calibrated indirectly through the methylene peak of adamantine observed at 28.8 ppm relative to tetramethylsilane at 0 ppm.

2.5. ^{13}C Dipolar decoupling/magic angle spinning (DD/MAS) NMR spectroscopy

^{13}C DD/MAS NMR spectrum was recorded on a Chemagnetics CMX300 spectrometer measured with an approximately 1.8 ms 30 ° pulse length and 10 s pulse sequence recycle time. In these experiments the sample was also spun at 3 kHz. The measurement was carried out on a 10 wt% solution of sample **2-B** in D_2O with at 25 °C, operating at 75.6 MHz for ^{13}C observation.

2.6. Deuterium 2D T_1-T_2, T_2-T_2 correlation experiments

All of the relaxation experiments were carried out on a Varian Unity 200 MHz NMR spectrometer with a liquids probe. The radio frequency pulse sequences for the T_1-T_2 and T_2-T_2 experiments used in this study are illustrated in Fig. 1 [31−33]. The deuterium 90 ° pulse length was calibrated to 35 ms; the effect of this pulse width on the measured spin dynamics is negligible as the measured relaxation times were on the order of milliseconds. For the PAD sample **2-B** the T_1-T_2 experiments were conducted at 20, 30, 40, 50, 60, and 70 °C. Additionally, T_2-T_2 exchange experiments were performed on PAD sample **2-B** at 70 °C. Temperature throughout all studies was maintained within 2 °C. In the T_1-T_2 experiment shown in Fig. 1 the magnetization is inverted by the initial 180 ° pulse and then recovers to thermal equilibrium during the variable delay t1 by relaxation time T_1. The 90 ° pulse following the delay t1 rotates the magnetization into the transverse

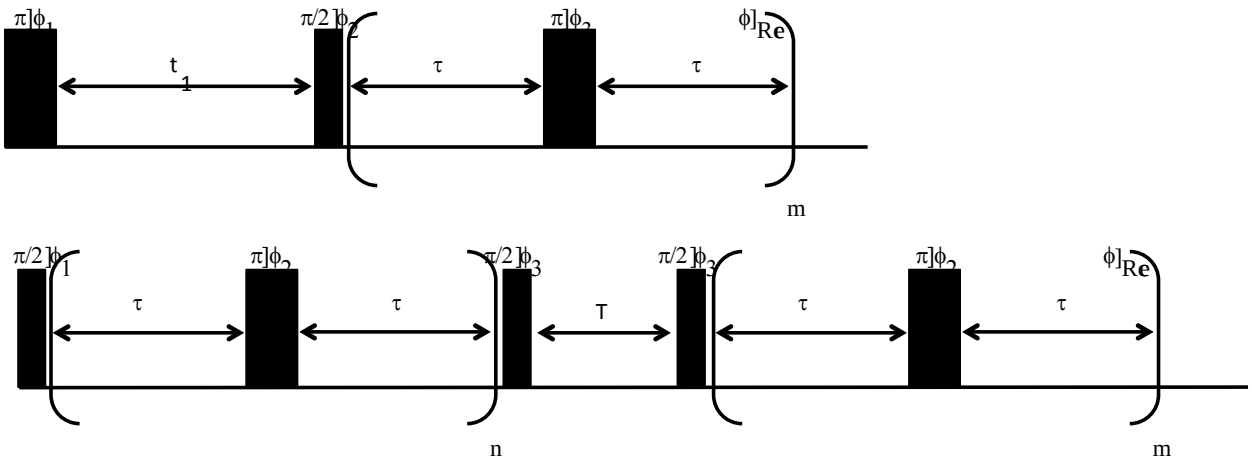

Fig. 1. Top) Radio frequency pulse sequence used for the 2D T_1−T_2 correlation experiments in this work; the phase cycling used was φ_1 = {x, −x}, φ_2 = {x, x, −x, −x}, and the receiver phase was φ_{Rec} = {x, x, −x, −x}. In the experiment, the π pulses where toggled as φ_3 = {y, −y}. The details regarding the experimental values for m, t1 and s are described in the text. Bottom) Radio frequency pulse sequence used for the 2D T_2−T_2 exchange measurements in this work; the phase cycling used was φ_1 = {x, −x}, φ_3 = {x, x, −x, −x} and the receiver phase was $\varphi_{1\mathrm{Rec}}$ = {x, −x}. The π pulses were toggled using the phase scheme φ_2 = {y, −y} and experimental values for time τ, the variables *n* and *m*, and the exchange time *T* are described in the text.

plane and the NMR signal is stroboscopically detected with a Carr−Purcell−Meiboom−Gill (CPMG) pulse train with s set to 0.350 ms. [42]. Using a 2D ILT of the data, a T_1−T_2 correlation map is obtained. In the T_2−T_2 experiment an initial CPMG pulse train is applied by varying the number of applied 180 ° pulses denoted *m* in Fig. 1. Following the initial CPMG pulse train a 90 ° pulse is applied to store the magnetization along the azimuthal axis for a time *T*. After the variable storage time *T*, the nuclear spins are again returned to the transverse plane and the T_2 is measured with a stroboscopically detected CPMG train. Different than the T_1−T_2 correlation experiment, this approach correlates T_2 relaxation times and allows for the probing of exchange between reservoirs distinguishable on the NMR time scale; water molecules exchanging between reservoirs correspond to cross peaks in the resulting T_2−T_2 ILT map. In the T_1−T_2 experiments t1 was logarithmically incremented from 1 ms to 10 s in 100 steps to enable an accurate measurement of T_1 values from 10 ms to 1 s and m = 6000 points were stroboscopically collected for the T_2 measurement. In the T_2−T_2 experiments the number of loops denoted n in the first CPMG train varied logarithmically from 1 to 6000 in 100 steps, and in the second dimension m = 6000 points were stroboscopically detected. In all experiments 16 scans were accumulated with a recycle delay of 10 s.

3. Results and discussion

3.1. Physical properties

The viscosity of 10 wt% aqueous solution **2** was measured in the temperature range of 10 ˚C−65 ˚C (Fig. 2). The viscosity of the polymer solution with a higher content of LA as a hydrophobic alkyl group increased at lower temperature, and the maximum observed viscosity was higher than in other samples studied. On the other hand, the polymer solution with low content of LA such as sample **2-E** did not show a strong thermo-responsive behavior. The 10 wt% aqueous solution of polymer sample **2-B** showed a significant increase in viscosity around 40 ˚C and the maximum viscosity of this polymer solution was approximately 70 Pa·s at 58 ˚C. With further heating the viscosity of sample **2-B** decreased gradually and the observed thermo-responsive behavior was reproducible as the heating and cooling processes were repeated. Subsequent elucidation of the thermo-responsive behavior was carried out on sample **2-B**.

3.2. Assignment of ^{13}C NMR spectra of PAD

The assignment of ^{13}C NMR spectra of sample **2-B** in D_2O refers to previous chapter.

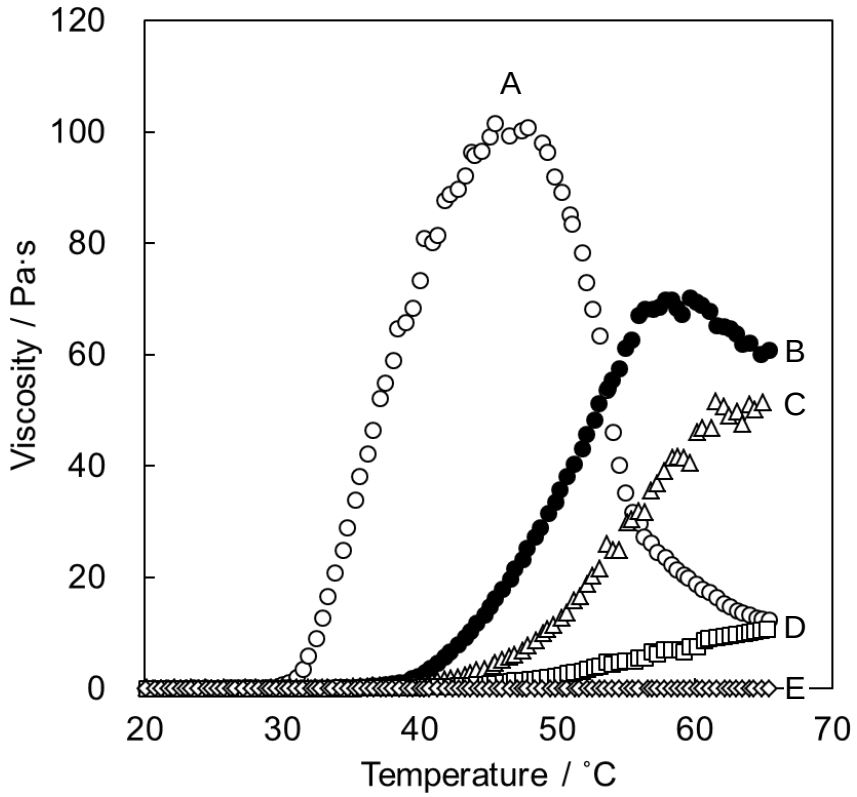

Fig. 2. Temperature dependence of the viscosity of 10 wt% aqueous solutions of PAD. Sample **2**; (A) LA/AP = 25/75, (B) LA/AP = 20/80, (C) LA/AP = 15/85, (D) LA/AP = 10/90, (E) LA/AP = 5/95. The rheometry measurements were carried out at a frequency of 1.0 Hz at a heating rate of 2.0 ˚C/min.

3.3. Structural change of thermo-responsive PAD with heating

In general, ^{13}C CP/MAS NMR peaks can be observed when strong nuclear spin dipolar interactions between carbons and protons exist. The observation of a high signal intensity in the ^{13}C CP/MAS NMR spectra indicates restricted or anisotropic motion of $^{1}H-^{13}C$ dipolar interactions, but weaker or no peaks may be due to a high degree of isotropic mobility and/or an increased separation between $^{1}H-^{13}C$ nuclear distances. Thus ^{13}C CP/MAS NMR is a powerful tool for elucidating dynamical and structural features of the restrained part of sample **2-B** in water. On the other hand the mobile component of sample **2-B** in water was observed by ^{13}C solution NMR methods. Thus both the ^{13}C CP/MAS NMR and ^{13}C solution NMR spectra were observed with a 10 wt% D_2O solution of sample **2-B** as a function of temperature to monitor the changes in the mobility of the PAD chain in aqueous solution.

The ^{13}C CP/MAS NMR spectra over a wide range of temperatures are shown in Fig. 3(A) together with ^{13}C DD/MAS NMR spectrum at 25 ˚C in Fig. 3(B).

Most of the peaks except for the carbonyl carbon in the hydrophilic amide group and the terminal methyl group in the LA side chain were observed in the ^{13}C CP/MAS NMR spectrum at 25 ˚C. Above 40 ˚C few ^{13}C CP/MAS NMR peaks could be observed except for small alkyl peak. On the other hand the ^{13}C solution NMR spectra were almost unchanged in both peak intensity and chemical shift (Fig. 4) over temperature range studied.

These experimental findings appear to indicate that PAD molecules in

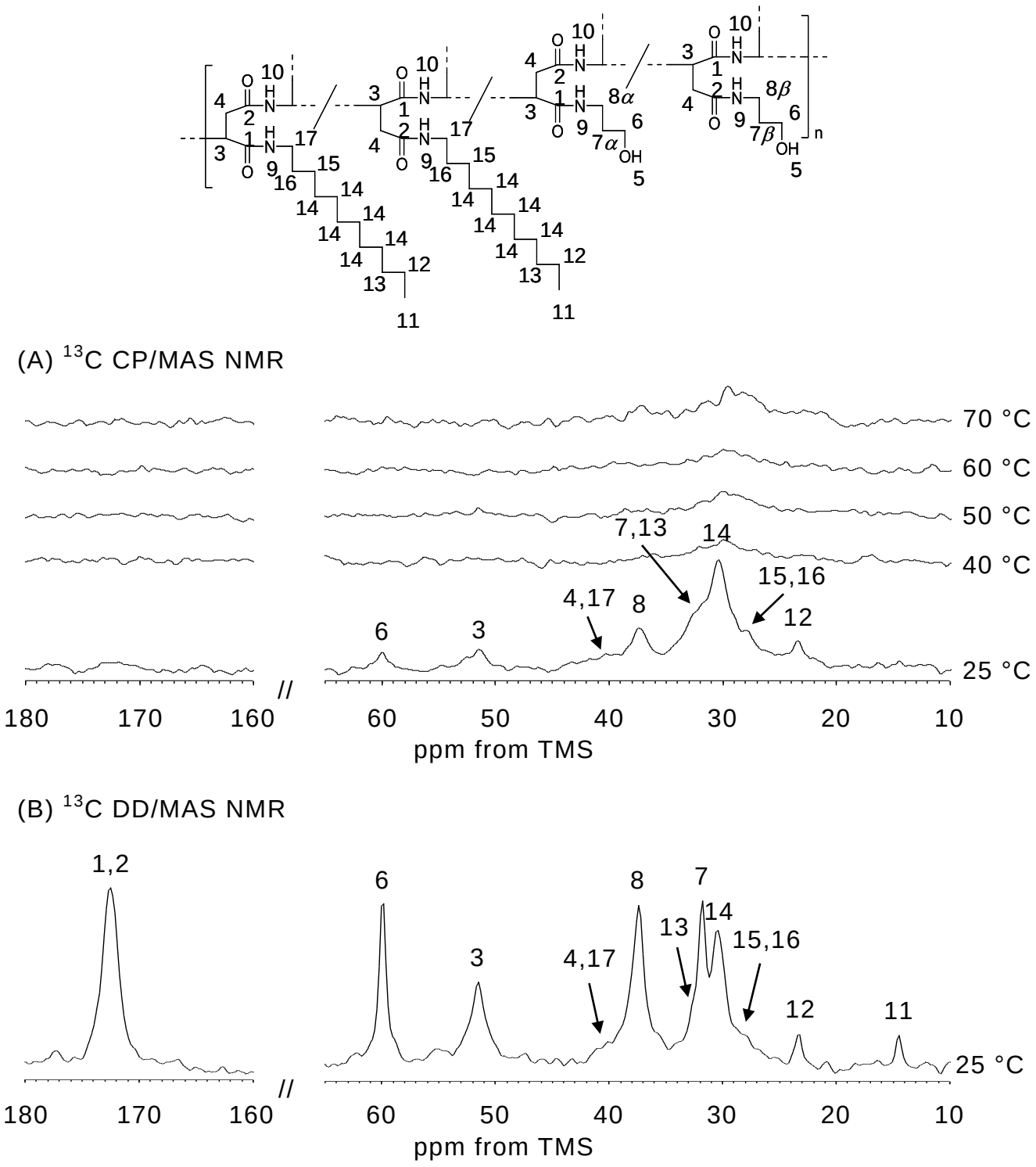

Fig. 3. (A) ^{13}C CP/MAS NMR spectra of PAD sample **2-B** in D_2O (10 wt%) as a function of temperature, and (B) ^{13}C DD/MAS NMR spectrum of PAD sample **2-B** in D_2O (10 wt%) at 25 ˚C used for spectral assignment.

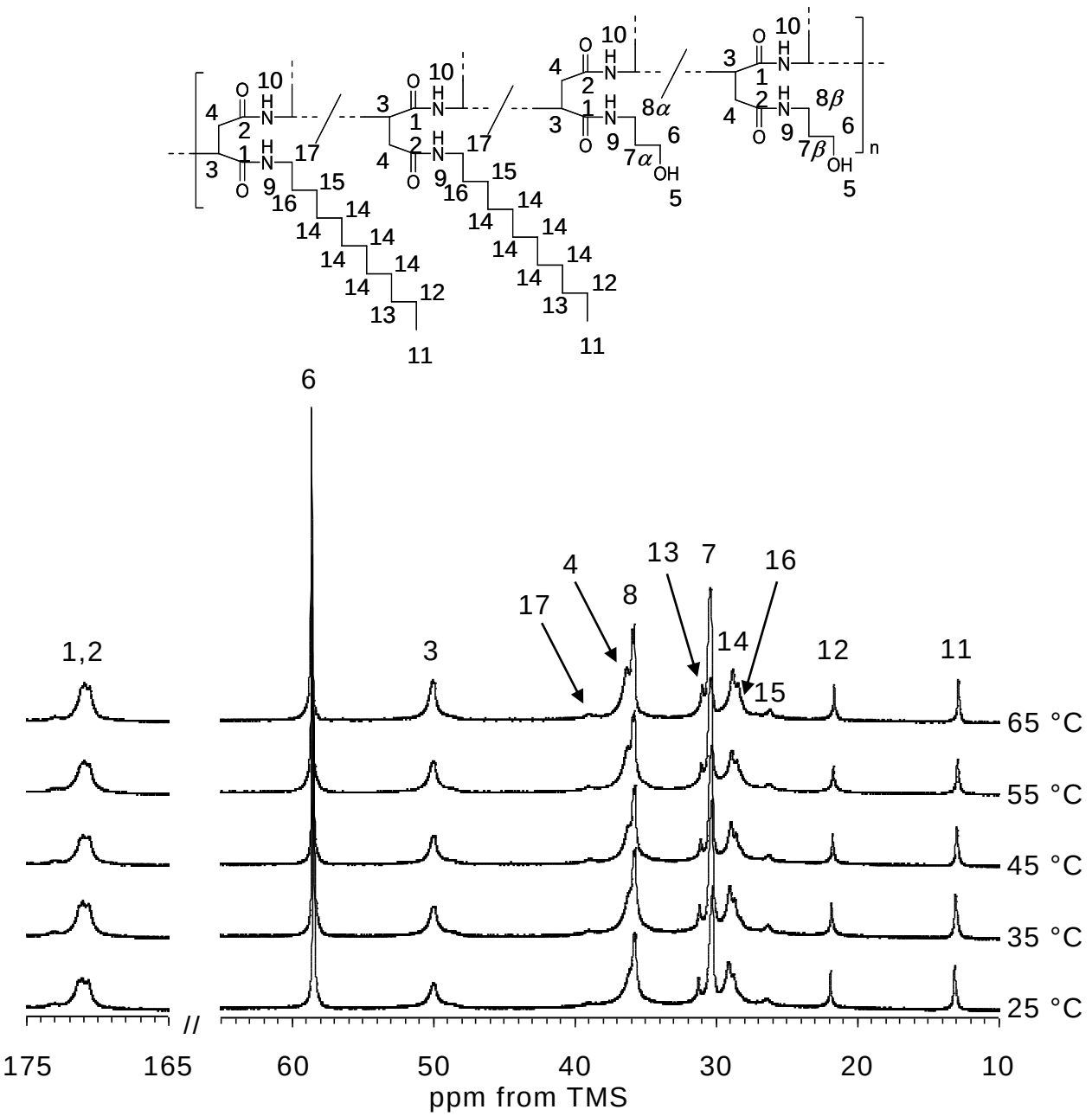

Fig. 4. ^{13}C solution NMR spectra of PAD sample **2-B** in D_2O (10 wt%) at various temperatures.

aqueous solution are in a highly mobile state over the observed temperature range even at 25 ˚C. Only at 25 ˚C were all the peaks from the PAD observed in the ^{13}C CP/MAS NMR spectra indicating the formation of strong interconnected polymer chains nodes, or polymer chains in very close proximity to one another. Increasing the temperature appears to result in a partial disentanglement of the nodes resulting from mobility or separation of the polymer chains and subsequent further heating results in little to no further structural variation.

3.4. Monitoring of the Water−PAD interaction

Deuterium T_1−T_2 and T_2−T_2 2D relaxation spectroscopies, using an ILT, were used to determine the dynamics, distribution, and exchange of waters of hydration to monitor the water−PAD interaction during the phase transition [31]. In the T_1−T_2 experiment the T_2 relaxation times of a system are measured as a function of separate inversion recovery experiments that probe the T_1 relaxation times. As described in ref 30, applying a 2D ILT of the experimental data the T_1 and T_2 NMR relaxation times are correlated and manifested into a peak in the 2D ILT map. The resulting 2D T_1−T_2 ILT maps at various temperatures are shown in Fig. 5.

Referring to Fig. 5, only one peak is observed in the T_1−T_2 map at 20 and 30 ˚C. At these temperatures $T_1 \cong T_2$ indicates that the deuterium nucleus undergoes nearly isotropic and unrestricted motion. However above 40 ˚C several peaks are revealed in the T_1−T_2 map indicating at least three distinguishable reservoirs of water with different dynamical characteristics

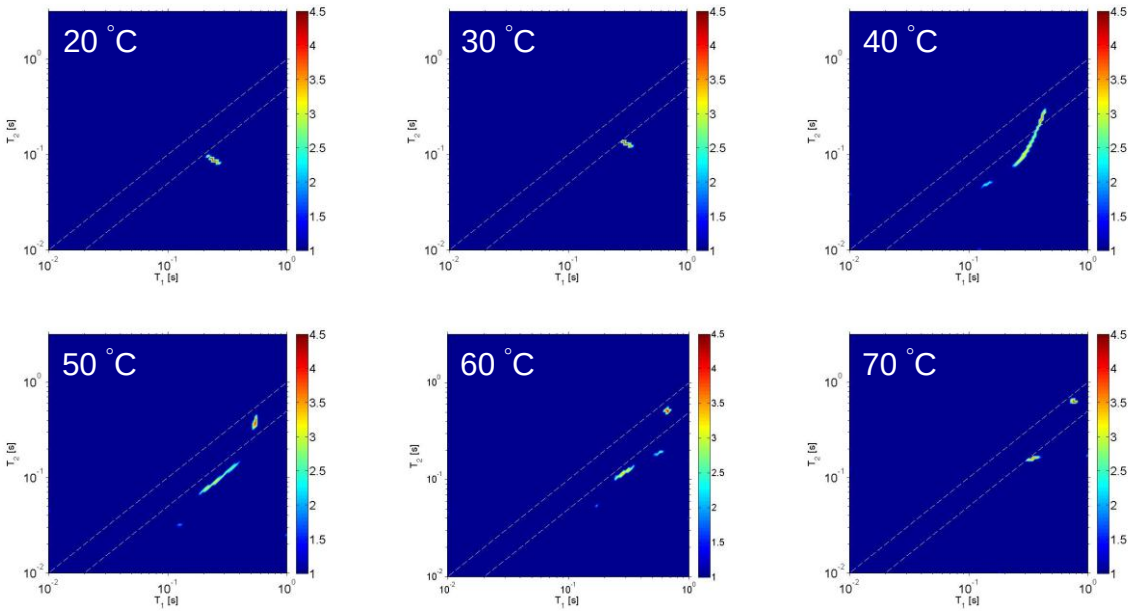

Fig. 5. Deuterium 2D T_1−T_2 ILT maps of PAD sample **2-B** in D_2O (10 wt%) as a function of temperature. The dashed lines in the images are intended to guide the eye for the region of the 2D map where T_1 is approximately equal to T_2. The signal intensity indicated by the color bar is on a logarithmic scale.

over the time scale of our measurement. For deuterium (spin I = 1) the $^2H-^2H$ and $^1H-^2H$ dipolar interactions are usually negligible relative to the quadrupolar interaction and the expressions for T_1 and T_2 are given by Ref. [43].

$$\frac{1}{T_1} = \frac{3}{40}\left(1+\frac{\eta^2}{3}\right)C_q\{J(\omega_D)+4J(2\omega_D)\}$$
$$\frac{1}{T_2} = \frac{1}{80}\left(1+\frac{\eta^2}{3}\right)C_q\{9J(0)+15J(\omega_D)+6J(\omega_D)\}$$

In the above expressions $C_q = \{[eQ/\hbar][\partial^2 V/\partial^2 z]\}^2$ is the quadrupolar coupling constant, h is the asymmetry parameter of the potential V (η = 0 for ^2H in water) and $J(\omega)$ is termed the spectral density function and is given by

$$J(\omega) = \frac{\tau_c}{1+(\omega\tau_c)^2}$$

In the spectral density function τ_c is termed the correlation time that characterizes the interaction of the nuclear quadrupolar moment with the electric field gradient. For the case of ^2H in D_2O the quadrupolar interaction is intramolecular in origin and the correlation time quantifies the tumbling nature of the molecule; a large correlation time corresponds to reduced tumbling motion of an individual water molecule. Using the above theoretical formalism the measured ratio of T_1 and T_2 allows for a determining the correlation time.

Table 1 summarizes the measured relaxation times at each temperature and the corresponding correlation times and relative proportions for each component observed in Fig. 5. Any peak in the 2D ILT map provides a distribution of T_1 and T_2 values. The entries in Table 1 following a ± symbol

Table 1. Summary of the measured T_1 and T_2 of the various components observed in the 2D T_1−T_2 ILT map of water in the PAD sample. As described in the text the correlation time (τ_c) is determined from the ratio of T_1 to T_2 and quantifies the tumbling of the D_2O molecule. The number following the ± symbol is not an error bar but expresses the distribution of T_1 and T_2 values in the 2D ILT map which is propagated into the computation of sc. In cases where the T_1−T_2 ILT map was broadly distributed (at 40 and 50 ˚C, refer to Fig. 3) the distribution value for T_1 and T_2 could not be accurately determined. The relative proportion was also determined based on the integrated signal intensity in the 2D T_1−T_2 ILT map at every temperature.

Temperature (˚C)	T_1 (s)	T_2 (s)	$\tau_c \times 10^{-9}$ (s)	Relative Proportion
20	0.247 ± 0.022	0.085 ± 0.005	6.78 ± 1.02	1
30	0.312 ± 0.016	0.129 ± 0.007	5.58 ± 0.68	1
40	0.413	0.245	3.45	0.976
	0.142 ± 0.014	0.048 ± 0.002	6.90 ± 0.96	0.024
50	0.546 ± 0.025	0.389 ± 0.042	2.50 ± 0.80	0.654
	0.259	0.096	6.29	0.346
60	0.658 ± 0.031	0.521 ± 0.029	1.95 ± 0.50	0.641
	0.572 ± 0.051	0.183 ± 0.009	7.29 ± 0.90	0.035
	0.285 ± 0.037	0.122 ± 0.020	5.36 ± 2.00	0.324
70	0.756 ± 0.036	0.658 ± 0.037	1.43 ± 0.57	0.643
	0.343 ± 0.033	0.163 ± 0.009	4.72 ± 0.92	0.357

should not be interpreted as experimental error bars but reflect the distribution of T_1 and T_2 values in a given peak in the 2D map. In addition the number shown for the correlation time following the ± symbol again are not to be interpreted as experimental error bars but are propagated from the distribution of T_1 and T_2 values. The correlation times were plotted against temperature in Fig. 6.

Our experimental data indicate that the measured correlation times are much larger than that of free water (free water has a correlation time on the order of 10^{-12} s at 20 ˚C). The reduced tumbling motion of the water molecule at any given temperature is due to the interaction with PAD chains that are present in the solution. The experimental data indicate a difference in mobility among the various sites at the different temperatures. One correlation time was obtained at 20 ˚C (6.78 ± 1.02 ns) and decreases when the temperature of the sample is raised to 30 ˚C (5.58 ± 0.68 ns) indicating an increase in the mobility of water molecules. However increasing the temperature to 40 ˚C several water reservoirs are observed with different correlation times which is the same temperature when the viscosity was observed to increase (Fig. 2). The correlation times at 40 ˚C are largely distributed and at 50 ˚C, the tendency is similar, but also separates into two groups. Specifically, we observe one short correlation time (2.5 ± 0.80 ns) and a second correlation time ranging between 6.0 and 7.0 ns. At 60 ˚C, the distribution is similar. Specifically, we observe one short correlation time (1.95 ± 0.50 ns) and a second group of water reservoirs having a correlation times between 5 and 7 ns. At 70 ˚C, the experimental T_1−T_2 map reveals only two water reservoirs. Even at this temperature where the viscosity of the sample is significantly

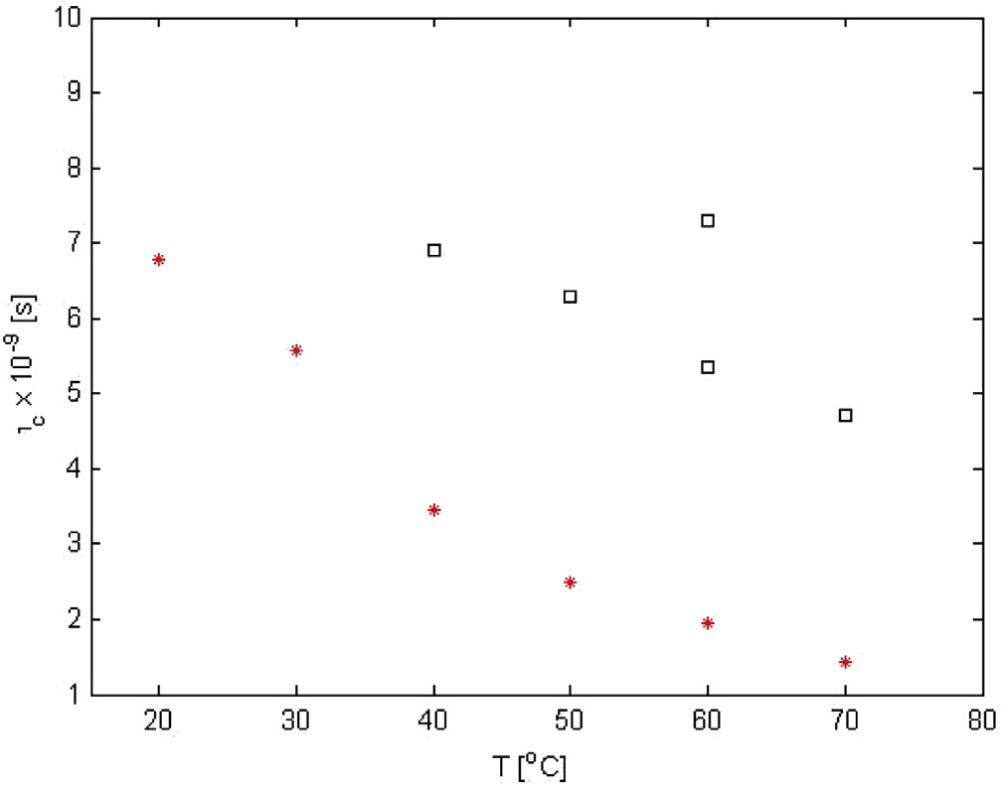

Fig. 6. Measured correlation times of water in PAD sample **2-B** (10 wt%) as a function of temperature. The figure is replicates the information tabulated in Table 1 which is determined from the T_1 and T_2 values in Fig. 3 with the error bars removed for clarity. One component of the water (red stars) observed in the 2D ILT maps is observed at all temperatures characterized by a correlation time that decreases monotonically with increasing temperature. At 40, 50, 60, and 70 ˚C at least two components of water are revealed (black squares).

higher than that at room temperature, we find that the correlation times of the water molecules differ by approximately a factor of 3 (1.43 ± 0.57 and 4.72 ± 0.92 ns).

The plots of the smallest τ_c value against temperature show a monotonic decrease (Fig. 6, red stars) which indicates an increase in the mobility of one of the reservoirs; the fraction of these component was constant, 0.65 between 50 ˚C and 70 ˚C. From 60 ˚C to 70 ˚C, two τ_c values decrease, which appears to be correlated to the decrease in the viscosity shown in Fig. 2. The most interesting phenomena is the appearance of the groups with larger τ_c values at 40 ˚C compared with the τ_c value at 30 ˚C. This corresponds to large increase in viscosity in Fig. 2 which persists until 50 ˚C. Thus, the behavior of the large correlation times of water appears to be correlated to the observed changes in viscosity from 40 ˚C to 70 ˚C. It should be pointed out that at 40 ˚C and 50 ˚C the T_1−T_2 maps were widely distributed (Fig. 5) due to a broad range of measured T_1 and T_2 values resolved by the ILT approach. As a consequence an accurate measurement of the T_1 and T_2 values and τ_c were not possible for one component at these temperatures.

Fig. 7 highlights the measurements of the T_2−T_2 exchange experiments performed at 70 ˚C on the PAD sample **2-B**. As discussed earlier this experimental approach allows for probing exchange between sites; exchange between two reservoirs with distinguishable T_2 relaxation times result in cross peaks in the resulting 2D ILT map. In Fig. 7 we show experimental measurements where the exchange time T (Fig.1) was varied from 0.5 ms to 270.0 ms. Our experimental data indicate that the two sites do not exchange over the time scale probed (experimentally many intermittent times as well as

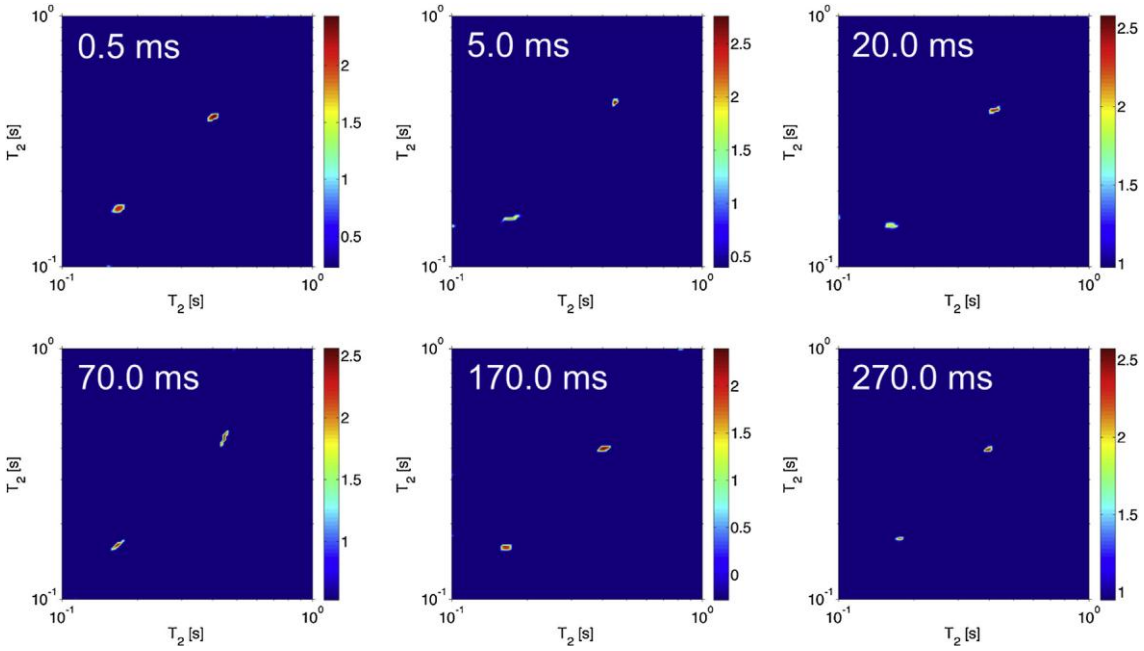

Fig. 7. Deuterium 2D ILT map of the T_2–T_2 exchange measurements performed at 70 ˚C of PAD sample **2-B** in D_2O (10 wt%). In the results shown the mixing time *T* (refer to Fig. 1) was experimentally varied from 0.5 ms to 270.0 ms. As discussed in the text the observation of a cross peak would indicate exchange between the two sites, however none was observed over the exchange times probed. The signal intensity in all cases indicated by the color bar is on a logarithmic scale.

for times less than 0.5 ms and greater than 270.0 ms were studied, however no cross peaks were observed).

Referring to Fig. 2, 40 ˚C corresponds to the temperature where the aqueous PAD sample exhibits a large change in viscosity. As discussed earlier, at this temperature the ^{13}C CP/MAS NMR data indicated partial disentanglement of the nodes by thermal agitation of the polymer chains. In addition at temperatures up to 60 ˚C, the aggregates disentangle and expand by activated molecular mobility and many reservoirs characterized by water having different dynamical characteristics are observed. By further heating the T_1-T_2 and T_2-T_2 the experimental data suggest that the PAD aqueous solution appears to divide into two phases between the restrained water in the polymer rich phase and the water which is removed from the polymer phase at 70 ˚C.

3.5. Proposed behavior of thermo-responsive PAD

A cartoon of the thermo-responsive behavior of the amphipathic PAD aqueous solution revealed by the ^{13}C CP/MAS NMR, ^{13}C solution NMR, and 2D T_1-T_2 and T_2-T_2 NMR results is schematically depicted in Fig. 8.

At temperatures near 20 ˚C the PAD molecules are dispersed homogeneously in an aqueous media although some chains form nodes; these aggregates are also uniformly dispersed in water. At this temperature water molecules exhibit only one dynamical characteristic as evidenced by a single T_1 and T_2 relaxation times highlighted in Fig. 5. Molecular mobility is activated with increasing temperature above 20 ˚C resulting in

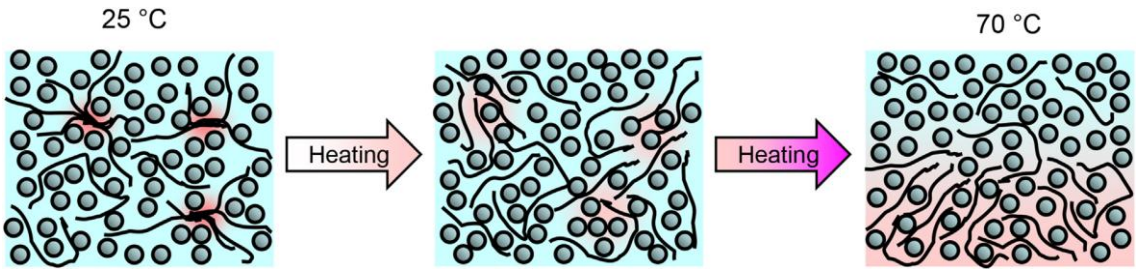

Fig. 8. A cartoon representation highlighting the thermal behavior of the aqueous PAD as a function of temperature. In the figure, spheres denote water molecules, black lines denote PAD chains and red is used to indicate restricted motion of the polymer chains due to inter-chain interactions, such as nodes. As described in the text, near 20 ˚C polymer chain nodes are present and surrounding water has only one nearly isotropic dynamical characteristic over the time scale of the measured T_1 and T_2 relaxation times (refer to Fig. 3). With increasing temperature polymer chain nodes are broken due to thermal agitation resulting in the formation of a gel characterized by a network of PAD molecules with at least three interspersed reservoirs of water characterized by different dynamical characteristics (refer to Fig. 3). At 70 ˚C only two water reservoirs are observed that do not exchange (refer again to Figs. 3 and 5).

disentanglement and expansion of the aggregates; solid-like structures present at 20 ˚C disappear as evidenced by the reduction of the ^{13}C CP/MAS signal when the temperature was increased from 25 ˚C to 70 ˚C highlighted in Fig. 3(A).

One simple physical picture of a gel involves connected polymer chains that entrap a fluid. Near 40 ˚C several peaks are observed in the deuterium 2D T_1−T_2 map indicating different water reservoirs characterized by distinguishable dynamical characteristics; at this temperature the PAD would appear to form a complex network that encases surrounding water molecules. By subsequent heating above 60 ˚C molecular mobility is increased and the PAD network is divided into two phases between the restrained water which is captured into the polymer rich phase and the more mobile water which is removed from the polymer phase. Above 60 ˚C the viscosity of the polymer solution is reduced due to further thermal agitation resulting in a weakening of the polymer network that was formed in the gel state.

4. Conclusions

This chapter aimed to elucidate the behavior of a thermo-responsive amphiphilic poly(*N*-substituted α/β-asparagine) derivative that exhibits a significant viscosity change with increasing temperature in an aqueous solution. The detailed polymer structure at various temperatures was analyzed by ^{13}C solution and CP/MAS NMR techniques, and the dynamical characteristics and distribution of the surrounding waters of hydration were studied by 2D T_1-T_2 and T_2-T_2 NMR methodology. It is expected that detailed knowledge of this unique thermo-responsive behavior presented herein may allow for further enhancement of the thermo-responsive behavior as well as novel targeted applications.

References

[1] M. A. C. Stuart, W. T. S. Huck, J. Genzer, M. Müller, C. Ober, M. Stamm, G. B. Sukhorukov, I. Szleifer, V. V. Tsukruk, M. Urban, F. Winnik, S. Zauscher, I. Luzinov, S. Minko, *Nat. Mater.*, 9 (2010) 101.

[2] A. S. Hoffman, *Adv. Drug Deliv. Rev.*, 65 (2013) 10.

[3] M. Heskins, J. E. Guillet, *J. Macromol. Sci. Chem. Ed.*, A2 (1968) 1441.

[4] G. Chen, A. S. Hoffman, *Nature*, 373 (1995) 49.

[5] H. Uyama, S. Kobayashi, *Chem. Lett.*, (1992) 1643.

[6] M. Kurisawa, Y. Yokoyama, T. Okano, *J. Control. Release*, 68 (2000) 1.

[7] A. Tuncel, E. Ünsal, H. Çicek, *J. Appl. Polym. Sci.*, 77 (2000) 3154.

[8] Y. Guan, Y. Zhang, *Soft Matter*, 7 (2011) 6375.

[9] H. S. Kang, S. R. Yang, J.-D. Kim, S.-H. Han, I.-S. Chang, *Langmuir*, 17 (2001) 7501.

[10] Y. Tachibana, M. Kurisawa, H. Uyama, T. Kakuchi, S. Kobayashi, *Chem. Commun.*, (2003) 106.

[11] E. Watanabe, N. Tomoshige, *Chem. Lett.*, (2005) 876.

[12] Y. Takeuchi, H. Uyama, N. Tomoshige, E. Watanabe, Y. Tachibana, S. Kobayashi, *J. Polym. Sci. Part A Polym. Chem.*, 44 (2006) 671.

[13] E. Watanabe, N. Tomoshige, H. Uyama, *Macromol. Symp.*, 249−250 (2007) 509.

[14] M. Obst, A. Steinbüchel, *Biomacromolecules*, 5 (2004) 1166.

[15] J. R. Moon, Y. S. Jeon, D. J. Chung, D. Kim, J.-H. Kim, *Macromol.*

Res., 19 (2011) 515.

[16] A. Desjardins, A. Eisenberg, *Macromolecules*, 24 (1991) 5779.

[17] R. L. Xu, M. A. Winnik, F. R. Hallett, G. Riess, M. D. Croucher, *Macromolecules*, 24 (1991) 87.

[18] K. Mortensen, Y. Talmon, *Macromolecules*, 28 (1995) 8829.

[19] A. Jada, G. Hurtrez, B. Siffert, G. Riess, *Macromol. Chem. Phys.*, 197 (1996) 3697.

[20] B. Wittgren, K. G. Wahlund, H. Derand, B. Wesslen, *Macromolecules*, 29 (1996) 268.

[21] K. Akiyoshi, S. Deguchi, H. Tajima, T. Nishikawa, J. Sunamoto, *Macromolecules*, 30 (1997) 857.

[22] J. Kriz, B. Masar, J. Plestil, Z. Tuzar, H. Pospisil, D. Doskocilova, *Macromolecules*, 31 (1998) 41.

[23] M. Mizusaki, Y. Morishima, F. M. Winnik, *Macromolecules*, 32 (1999) 4317.

[24] J. A. Massey, K. Temple, L. Cao, Y. Rharbi, J. Raez, M. A. Winnik, I. Manners, *J. Am. Chem. Soc.*, 122 (2000) 11577.

[25] J. Schaefer, E. O. Stejskal, *Top. Carbon-13 NMR Spectrosc.*, 3 (1979) 283.

[26] I. Ando, T. Asakura, Ed., *Solid state NMR of polymers*, (1998) 1−1000, Elsevier, Amsterdam.

[27] H. N. Cheng, A. D. English, *NMR spectroscopy of polymers in solution and in the solid state*, ACS symposium series, vol. 834 (2003) Oxford University, Washington DC.

[28] H. N. Cheng, T. Asakura, A. D. English, *NMR spectroscopy of*

polymers: innovative strategies for complex macromolecules, ACS symposium series, vol. 1077 (2011) Oxford University, Washington DC.

[29] T. Asakura, A. Asano, Ed., *Special issue: NMR of polymers. Polymer J.*, 44 (2012) 733−917.

[30] Y.-Q. Song, L. Venkataramanan, M. D. Hurlimann, M. Flaum, P. Frulla, C. Straley, *J. Magn. Reson.*, 154 (2002) 261.

[31] J.-H. Lee, C. Labadie, Jr C. S. Springer, G. S. Harbison, *J. Am. Chem. Soc.*, 115 (1993) 7761.

[32] K. E. Washburn, P. T. Callaghan, *Phys. Rev. Lett.*, 97 (2006) 175502.

[33] L. Venkataramanan, Y.-Q. Song, M. D. Hürlimann, *IEEE T. Signal Proces.*, 50 (2002) 1017.

[34] M. D. Hürlimann, L. Venkataramanan, *J. Magn. Reson.*, 157 (2002) 31.

[35] M. D. Hürlimann, L. Burcaw, Y.-Q. Song, *J. Colloid Interface Sci.*, 297 (2005) 303.

[36] B. Hills, A. Costa, N. Marighet, K. Wright, *Appl. Magn. Reson.*, 28 (2005) 13.

[37] P. J. McDonald, J.-P. Korb, J. Mitchell, L. Monteilhet, *Phys. Rev. E*, 72 (2005) 011409.

[38] C. Sun, O. Mitchell, J. Huang, G. S. Boutis, *J. Phys. Chem. B*, 115 (2011) 13935.

[39] C. Sun, G. S. Boutis, *New J. Phys.*, 13 (2011) 025026.

[40] X. Ma, C. Sun, J. Huang, G. S. Boutis, *J. Phys. Chem. B*, 116 (2012) 555.

[41] T. Takahashi, H. Kawashima, H. Sugisawa, T. Baba, *Solid State Nucl. Mag.*, 15 (1999) 119.

[42] S. Meiboom, D. Gill, *Rev. Sci. Instrum.*, 29 (1958) 668.

[43] A. Abragam, *Principles of nuclear magnetism*, (1961) Oxford University, New York.

Chapter 5

Concluding Remarks

This thesis deals with the development and NMR studies of thermo-responsive polymer materials based on poly(asparagine) derivatives (PADs). The results obtained through this study summarized as follows;

In Chapter 2, new thermo-responsive and biodegradable PADs which show not only the lower critical solution temperature (LCST) but also a sol−gel−sol phase transition were developed. These thermo-responsive properties could be precisely controlled by changing the composition of the side chain in PAD. In addition, these characteristic phenomena of phase separation and gelation with increasing temperature were confirmed by DLS measurements and TEM images. In the case of PAD used *N*,*N*-dimethyl-1,3-propanediamine (DMPDA) as hydrophilic side chain, the micelle-like small aggregates at low temperature are assembling and forming larger aggregate with heating. The driving force of thermo-responsiveness in this DMPDA case is described by a conventional model which has been proposed. However, the thermo-gelation mechanism of the PAD with 1-amino-3-propanol (AP) as a hydrophilic group in water was quite different from that with DMPDA.

In chapter 3, the aqueous solution of thermo-responsive PAD with AP

side chain formed a hydrogel without any additives. This PAD in aqueous solution was characterized by using NMR techniques. The mobility of PAD molecules was reduced in water. In particular, the hydrophobic segment was extremely restricted as compared to the hydrophilic segment by strong hydrophobic interaction. At this time, a part of side chains derived from AP and laurylamine was changed from extended state to contracted state. Namely, this amphiphilic PAD forms a micelle like aggregation structure under water.

In chapter 4, the behavior of a thermo-responsive amphiphilic PAD with AP unit as hydrophilic side chain that exhibits a significant viscosity change with increasing temperature in an aqueous solution was elucidated by using relatively new NMR technique. The detailed polymer structure at various temperatures was analyzed by ^{13}C solution and CP/MAS NMR techniques, and the dynamical characteristics and distribution of the surrounding waters of hydration were studied by two-dimensional T_1-T_2 and T_2-T_2 NMR methodology. It is expected that detailed knowledge of this unique thermo-responsive behavior presented herein may allow for further enhancement of the thermo-responsive behavior as well as novel targeted applications.

In conclusion, the present unique thermo-responsive polymer materials based on PAD were proposed in this thesis. By using poly(succinimide) as the precursor, the tailor-made molecular design of poly(aspartic acid) was possible due to the facile introduction of various functional groups in the polymer chain. These studies are the new model design of the thermo-responsive polymer materials possessing high biocompatibility and biodegradability mainly suitable for the biomedical

applications like as injectable biomedical device, controlled release of drugs, tissue engineering, and others. In addition, relatively new NMR technique will be helpful to develop the future materials.

On the basis of this molecular design, further progression of applied researches of poly(amino acid) based smart material is expected in future.

List of Publications

[1] "Preparation and Physical Properties of Thermoresponsive Biodegradable Poly(asparagine) Derivatives"

E. Watanabe, N. Tomoshige

Chem. Lett., (2005) 876−877.

DOI: 10.1246/cl.2005.876

[2] "New Biodegradable and Thermoresponsive Polymers Based on Amphiphilic Poly(asparagine) Derivatives"

E. Watanabe, N. Tomoshige, H. Uyama

Macromol. Symp., 249/250 (2007) 509−514.

DOI: 10.1002/masy.200750428

[3] "NMR Studies of Thermo-responsive Behavior of an Amphiphilic Poly(asparagine) Derivative in Water"

E. Watanabe, G. S. Boutis, H. Sato, S. Sekine, T. Asakura

Polymer, 55 (2014) 278−286.

DOI: 10.1016/j.polymer.2013.11.015

[4] "Characterization of Thermo-responsive Poly(asparagine) Derivative in Water"

E. Watanabe, H. Sato, S. Sekine, T. Asakura

in preparation.

Other Publications

[1] "Temperature-sensitive Poly(amino acid) Derivative"
N. Tomoshige, **E. Watanabe**, H. Shinoda, H. Yoshizawa
JP2003-147198A.

[2] "Humectant Comprising Temperature-sensitive Poly(amino acid) Derivative"
N. Tomoshige, **E. Watanabe**, K. Okumura
JP2004-359549A.

[3] "Injectable Thermoreversible Hydrogels Based on Amphiphilic Poly(amino acid)s"
Y. Takeuchi, H. Uyama, N. Tomoshige, **E. Watanabe**, Y. Tachibana, S. Kobayashi
J. Polym. Sci. Part A: Polym. Chem., 44 (2006) 671−675.
DOI: 10.1002/pola.21189

Acknowledgements

The present research was carried out from 2011 to 2014 at the Department of Biotechnology and Life Science, The Graduate School of Engineering, Tokyo University of Agriculture and Technology.

I would like to express my sincere gratitude to Professor Tetsuo Asakura of the Department of Biotechnology and Life Science, The Graduate School of Engineering, Tokyo University of Agriculture and Technology for his continuous guidance, encouragement, and supervision.

I would like to thank Professor Hiroshi Uyama (Division of Applied Chemistry, Graduate School of Engineering, Osaka University), Associate Professor Gregory S. Boutis (Department of Physics, Brooklyn College, The City University of New York), Mr. Naoki Tomoshige (Mitsui Chemicals Inc.), Dr. Sokei Sekine, and Mrs. Hiroko Sato (Mitsui Chemical Analysis & Consulting Service, Inc.) for their valuable advices and instructive comments.

I am also grateful to Dr. Shinji Ogawa, Mr. Takayasu Ikeda, and Mr. Yoshikazu Uehara who willingly accepted my challenge and watched patiently without disturbing.

Finally, I wish to express heartily thanks to Yuko, Hayato, Tatsuki, Satotsugu, Hideko, Tomoko, Keiko, and Reiko who encouraged and supported my study.

September 2014

Eiji Watanabe